

1 **Total sulphate vs. sulphuric acid monomer in nucleation** 2 **studies**

3

4 **K. Neitola¹, D. Brus^{1,2}, U. Makkonen¹, M. Sipilä³, R. L. Mauldin III^{3, 4}, N. Sarnela³,**
5 **T. Jokinen³, H. Lihavainen¹ and M. Kulmala³**

6 [1] {Finnish Meteorological Institute, Erik Palménin aukio 1, P.O. Box 503, 00100 Helsinki,
7 Finland}

8 [2] {Laboratory of Aerosol Chemistry and Physics, Institute of Chemical Process Fundamentals
9 Academy of Sciences of the Czech Republic, Rozvojová 135, 165 02 Prague 6, Czech
10 Republic}

11 [3] {Department of Physical Sciences, University of Helsinki, P.O. Box 64, 00014 Helsinki,
12 Finland}

13 [4] {Institute for Arctic and Alpine Research, University of Colorado, Boulder, CO 80309,
14 USA}

15 Correspondence to: K. Neitola (kimmo.neitola@fmi.fi)

16

17 **Abstract**

18 Sulphuric acid is known to be a key component for atmospheric nucleation. Precise
19 determination of sulphuric acid concentration is a crucial factor for prediction of nucleation
20 rates and subsequent growth. In our study, we have noticed a substantial discrepancy between
21 sulphuric-acid monomer and total-sulphate concentrations measured from the same source of
22 sulphuric-acid vapour. The discrepancy of about one-to-two orders-of-magnitude was found
23 with similar particle-formation rates. To investigate this discrepancy, and its effect on
24 nucleation, a method of thermally controlled saturator filled with pure sulphuric acid (97 % wt.)
25 for production of sulphuric-acid vapour is applied and rigorously tested. The saturator provided
26 an independent vapour-production method, compared to our previous method of the furnace
27 (Brus et al., 2010 and 2011), to find out if the discrepancy is caused by the production method
28 itself. The saturator was used in a sulphuric acid-water nucleation experiment, using a laminar

1 flow tube to check reproducibility of the nucleation results with the saturator method, compared
2 to the furnace. Two independent methods of mass spectrometry and online ion chromatography
3 were used for detecting sulphuric acid or sulphate concentrations. Measured sulphuric-acid or
4 total sulphate concentrations are compared to theoretical predictions calculated using vapour
5 pressure and a mixing law. The calculated prediction of sulphuric-acid concentrations agrees
6 very well with the measured values when total sulphate is considered. Sulphuric-acid monomer
7 concentration was found to be about two orders-of-magnitude lower than theoretical
8 predictions, but with a similar temperature dependency as the predictions and the results
9 obtained with the ion-chromatograph method. Formation rates are reproducible when compared
10 to our previous results with both sulphuric-acid or total-sulphate detection and sulphuric-acid
11 production methods separately, removing any doubts that the vapour-production method would
12 cause the discrepancy. Possible reasons for the discrepancy are discussed and some suggestions
13 include that the missing sulphuric acid is in clusters, formed with contaminants found in most
14 laboratory experiments. One-to-two orders-of-magnitude higher sulphuric-acid concentrations
15 (measured as total sulphate in this study) would contribute to a higher fraction of particle growth
16 rate than assumed from the measurements by mass spectrometers (i.e. sulphuric-acid
17 monomer). However, the observed growth rates by sulphate-containing vapour in this study
18 does not directly imply similar situation on field, where the sources of sulphate are much more
19 diverse.

20

21 **1 Introduction**

22 Secondary particle formation by gas-to-liquid conversion is widely recognized as an important
23 source of aerosol particles in the atmosphere worldwide (Weber et al., 1996; Kulmala et al.,
24 2004; Spracklen et al., 2006). These particles may grow to larger sizes and affect the radiative
25 balance of the earth by scattering and absorbing incoming radiation (Feingold and Siebert,
26 2009). Model calculations and observations suggest that new particle formation events with
27 subsequent growth can contribute a substantial amount to Cloud Condensation Nuclei (CCN)
28 concentrations, which can alter the lifetime and albedo of clouds (Lihavainen et al., 2003 and
29 2009; Merikanto et al., 2009). Furthermore, aerosols can reduce visibility and have potential
30 health effects (Davidson et al., 2005).

31 Significant effort has been made by field measurements and laboratory studies, together with
32 computer simulations, to understand the particle-formation mechanism itself and the

1 atmospheric conditions involved in the gas-to-liquid conversion. Despite such effort and
2 numerous results, the underlying mechanism is not yet found.

3 It is widely accepted that sulphuric acid plays a key role in atmospheric nucleation (Kulmala et
4 al., 2006; Sipilä et al., 2010; Brus et al., 2011; Kirkby et al., 2011). Binary nucleation of
5 sulphuric acid and water (Vehkamäki et al., 2002; Yu, 2006; Kirkby et al., 2011), ternary
6 nucleation involving also ammonia and/or amines (Ball et al., 1999; Korhonen et al., 1999;
7 Napari et al., 2002; Benson et al., 2009; Berndt et al., 2010; Kirkby et al., 2011; Zollner et al.,
8 2012) and ion-induced nucleation (Lee et al., 2003; Lovejoy et al., 2004; Yu et al., 2008, 2010;
9 Nieminen et al., 2011) have been suggested as possible mechanisms for nucleation to occur in
10 the atmosphere. Ions have been shown to lower the thermodynamic potential of nucleation
11 (Arnold 1980; Winkler et al., 2008; Kirkby et al., 2011), but the role of ions in nucleation
12 occurring in atmospheric boundary layer has been shown to be minor (Manninen et al., 2010;
13 Paasonen, et al., 2010, Kerminen et al., 2010; Hirsikko et al., 2011).

14 Recently several laboratory studies have been conducted concerning the role of sulphuric acid
15 in atmospheric nucleation (e.g. Benson et al., 2008, 2011; Young et al., 2008; Berndt et al.,
16 2008, 2010; Brus et al., 2010, 2011; Sipilä et al., 2010; Kirkby et al., 2011; Zollner et al., 2012)
17 with different methods of producing the gas phase sulphuric acid: with their own advantages
18 and disadvantages. For example, the evaporation method of weak sulphuric-acid solution used
19 by Viisanen et al. (1997) and Brus et al. (2010 and 2011) introduces a thermal gradient.
20 Production of sulphuric acid with a $\text{SO}_2 + \text{OH}$ reaction is used in most of the experiments, since
21 it is similar to that observed in atmosphere (e.g. Benson et al., 2008; Berndt et al., 2008, 2010;
22 Sipilä et al., 2010; Kirkby et al., 2011). The SO_2 oxidation method involves the use of UV light
23 to produce OH radicals. The excess OH must be removed so that it does not disturb the
24 nucleation process itself (Berndt et al., 2010). Another way is to have excess SO_2 , so that all
25 the OH reacts rapidly with SO_2 ; but for the calculation of the produced H_2SO_4 concentration,
26 the exact concentration of OH produced must be known (Benson et al., 2008). Ball et al., (1999)
27 and Zollner et al., (2012) produced sulphuric acid vapour by saturating N_2 flow in a glass
28 saturator-containing pure (~96 % and ~98 %, respectively) sulphuric acid. Ball et al., (1999)
29 varied the temperature of the saturator, whilst Zollner et al., (2012) kept the saturator at constant
30 temperature (303 K) and varied the carrier-gas flowrate to change the sulphuric acid
31 concentration.

1 As stated by others in literature (e.g. Benson et al., 2011; Brus et al., 2011; Kirkby et al., 2011),
2 contaminants are present in most of the laboratory nucleation studies. These contaminants arise
3 from different sources, such as from the water used for humidifying the carrier gas or from the
4 carrier gas itself which contains trace levels of contaminants. It is almost impossible to remove
5 these contaminants, which most probably affect the nucleation process itself.

6 Brus et al. (2011) reported a discrepancy in sulphuric-acid mass-balance between a known
7 concentration of weak sulphuric-acid solution introduced to the experimental setup and a
8 measured sulphuric-acid concentration, even though correction for wall losses and losses to
9 particle-phase was applied, one-and-half orders-of-magnitude difference in sulphuric acid
10 concentration was found (see Fig. 5 in Brus et al., 2011). A large discrepancy between measured
11 sulphuric-acid monomer and total-sulphate concentration was observed in the present study too.
12 To investigate the reason for this discrepancy, we applied a thermally controlled saturator (e.g.
13 Wyslouzil et al., 1991; Ball et al., 1999) to produce sulphuric-acid vapour. The output of the
14 saturator was tested with two independent detection methods (mass spectrometry and ion
15 chromatography) before using the saturator in a sulphuric acid-water nucleation study in a
16 laminar flow tube.

17 Applying the saturator as the source of the sulphuric-acid vapour made it possible to compare
18 the saturator to the furnace, which was used as the source of the sulphuric acid previously (Brus
19 et al., 2010 and 2011) and eliminate the production method as a reason for the discrepancy. The
20 flow-tube measurements with the saturator and the two sulphuric-acid or total-sulphate
21 detection methods were conducted to check reproducibility of particle formation rates between
22 the saturator and the furnace, with similar observed sulphuric-acid or total-sulphate
23 concentrations. The measured sulphuric-acid or total-sulphate concentrations were compared
24 and the total losses of sulphuric acid or sulphate were determined for both mass spectrometers
25 and the ion chromatograph. The level of ammonia contaminant in the system was determined
26 with the ion-chromatograph method.

27

28 **2 Experimental**

29 The measurement setup presented here is partially introduced in Brus et al. (2010), and only the
30 main principle of the method and the most substantial changes are described here. The setup
31 for testing the output of the saturator with two independent sulphuric-acid or total-sulphate

1 detection methods is described. The instrumentation for sulphuric-acid or total-sulphate and
2 freshly-formed-particle detection is shortly presented.

3 **2.1 Saturator**

4 The saturator was a horizontally placed cylinder made of iron with Teflon insert inside the
5 cylinder (inner diameter, I.D., of 5 cm). It was thermally controlled with a liquid-circulating
6 bath (LAUDA RC 6) and the temperature was measured just above the liquid surface with a
7 calibrated PT100 probe (accuracy ± 0.05 K) inserted from the outlet side of the saturator (Fig.
8 1). The saturator was filled with 150-200 ml of pure sulphuric acid (~97 % wt., Baker analyzed).
9 H₂SO₄ vapour was produced by flowing purified, dry, particle-free carrier gas through the
10 saturator in the range of 0.05-1 litres per minute (lpm) saturating the flow with vapour according
11 to the temperature of the saturator. Carrier gas flows were purified in all experiments first with
12 activated carbon capsules (Pall Corp., USA) to remove all organic vapours via diffusion to the
13 surfaces and after with a HEPA filters (Pall Corp. USA) to remove any particles left in the flow.
14 The saturator flow was thermally controlled to the same temperature as the saturator before
15 entering it, to ensure temperature stability inside the saturator.

16 The theoretical prediction of sulphuric-acid vapour concentration was calculated using the
17 equation for vapour pressure from Kulmala and Laaksonen (1990) which uses the
18 measurements by Ayers et al. (1980) and theoretically extrapolates the vapour pressure to lower
19 range of temperatures used in this study:

$$20 \quad \ln p = \ln p_0 + \frac{\Delta H_v(T_0)}{R} \times \left[-\frac{1}{T} + \frac{1}{T_0} + \frac{0.38}{T_c - T_0} \times \left(1 + \ln \frac{T_0}{T} - \frac{T_0}{T} \right) \right], \quad (1)$$

21 where p is the vapour pressure (atm), $p_0 = - (10156 / T_0) + 16.259$ atm (Ayers et al., 1980), T is
22 the temperature, T_c is critical temperature, 905 K, and T_0 is chosen to be 360 K so $\Delta H_v(T_0) / R$
23 = 10156. See Kulmala and Laaksonen (1990) for more details. Here the predicted sulphuric-
24 acid concentration depends only on saturator temperature, flowrate through the saturator and
25 mixing flow. Measured sulphuric-acid or total-sulphate concentration is compared also to
26 empirical fit by Richardson et al. (1986):

$$27 \quad \ln p = 20.70 - \frac{9360}{T} . \quad (2)$$

1 The fit is made to their measurement data in the temperature range of 263.15-303.15 K, which
2 suits the temperature range of the present study.

3 **2.2 Setup for testing saturator with mass spectrometers and online ion** 4 **chromatograph**

5 The saturator was tested in two different tests. First with mass spectrometers: Chemical
6 Ionization Mass Spectrometer (CIMS) (Eisele and Tanner, 1993; Mauldin et al., 1998; Petäjä
7 et al., 2009) and Atmospheric Pressure interface Time Of Flight mass spectrometer, (CI-Api-
8 TOF, Tofwerk AG, Thun, Switzerland and Aerodyne Research Inc., USA; Junninen et al.,
9 2010) with a similar Chemical Ionization inlet as the CIMS (Jokinen et al., 2012). A second test
10 was done with the instrument for Measuring AeRosols and GAses (MARGA, Metrohm
11 Applikon Analytical BV, Netherlands; ten Brink et al., 2007). Both measurements were
12 performed with the same setup (Fig. 1). The flow from the saturator (0.5 lpm) was mixed with
13 another flow of the same gas (20 or 40 lpm) after the saturator to meet the inlet flows of the
14 instruments. The relative humidity (RH) was set by 2 or 3 Nafion humidifiers (MD-series,
15 Perma pure, USA) and monitored from the excess flow. The design of the inlet system for
16 mixing the different flows and flow schematics to the instruments can be found in the
17 supplementary material (Fig. S2). Different configurations after the mixing were tested and no
18 difference in the observed concentration was found. The temperature of the saturator was
19 increased in 5-degree steps from approximately 273 K to 303 K (MARGA) and 313 K (CIMS
20 and CI-Api-TOF) in order to increase the sulphuric-acid concentration. The temperature was
21 kept constant from 2 to 8 hours in order to achieve a steady state. The measured sulphuric-acid
22 monomer and total-sulphate concentrations were compared to theoretical values calculated
23 from the vapour pressure of sulphuric acid using Eq. (1) and (2).

24 **2.3 Flow-tube setup for nucleation measurements**

25 The flow-tube setup consists of four main parts: a saturator, a mixing unit, a flow nucleation
26 chamber and detection of sulphuric acid or total sulphate and particles (Fig. 2). The sulphuric-
27 acid vapour is produced in the saturator and turbulently mixed with clean, particle-free carrier
28 gas in the mixing unit. Particles formed inside the saturator are lost in the 1-m long, thermally
29 controlled Teflon tube (I.D. 4 mm) before the mixer, by diffusion and by the turbulent mixing
30 in the mixer. After the mixing unit, nucleation and subsequent growth take place in the laminar
31 flow chamber. The flow chamber consists of two 100-cm-long stainless steel cylinders (I.D. 6

1 cm) connected with a Teflon piece (height 3.5 cm, I.D. 6 cm), positioned vertically and
2 thermally controlled with a liquid circulating bath (LAUDA RC 6). One of the 100-cm-long
3 parts of the flow chamber has four holes on the sides every 20 cm from the beginning of the
4 chamber. The 3.5-cm Teflon connector between the two 100-cm flow-tube pieces has also a
5 hole (see Fig. 2). These holes are used to continuously measure temperature in the flow tube
6 with PT100 probes to ensure constant desired nucleation temperature. The RH of the mixing
7 flow is controlled by 2 or 3 Nafion humidifiers. RH and temperature are measured also at the
8 end of the tube with Vaisala HMP37E and humidity data processor Vaisala HMI38. Both
9 saturator and mixing flow of the tube are controlled by a mass flowrate controller (MKS type
10 250) with an accuracy of $\pm 3\%$. Flowrates through the saturator for nucleation measurements
11 were kept at 0.13-0.27 lpm. The mixing flow was kept at approximately 11 lpm.

12 **2.4 H₂SO₄ monomer, sulphate and particle detection**

13 Gas phase sulphuric-acid monomers were measured with CIMS or CI-Api-TOF. The CI-inlet
14 used in both instruments works as follows: the sulphuric-acid molecules are ionized in ambient
15 pressure via proton transfer between nitrate ions (NO_3^-) and sulphuric acid molecules (H_2SO_4).
16 The nitrate ions are produced from nitric acid with radioactive ^{241}Am -source and mixed in a
17 controlled manner in a drift tube, using a concentric sheath and sample flows together with
18 electrostatic lenses.

19 After the ionization in the inlet, the instruments differ from each other. In the CIMS sample,
20 flow is dried using a nitrogen flow to dehydrate the molecules before entering the vacuum
21 system and detection in the quadrupole mass spectrometer. In the CI-Api-TOF, a flowrate of
22 0.8 lpm is guided through a critical orifice. The ions are guided through the differentially
23 pumped Atmospheric pressure interface (Api) and finally to the TOF for detection according to
24 the ions' mass-to-charge ratio.

25 The monomer concentration is determined by the ratio of the resulting ion signals (HSO_4^- and
26 $\text{HSO}_4^- \cdot \text{HNO}_3$) and the reagent ion signals (NO_3^- , $\text{HNO}_3 \cdot \text{NO}_3^-$ and $(\text{HNO}_3)_2 \cdot \text{NO}_3^-$). This ratio is
27 then multiplied by the instrument-dependent calibration factor in both instruments. The
28 calibration factor used here was $5 \cdot 10^9$ for both instruments. Neither CIMS nor CI-Api-TOF was
29 calibrated using the saturator setup, but instead before the experiments using the standard
30 calibration procedure of oxidation of SO_2 with OH (Kürten et al., 2012). For more information
31 about the calibration of CIMS, see Berresheim et al. (2000), Petäjä et al. (2009), Zheng et al.

1 (2010) and Kürten et al. (2012). The nominal sample flowrate of these instruments is ~10 lpm.
2 We considered only the monomer concentration, although detection of dimers and even larger
3 clusters of pure sulphuric acid is possible with CI-API-TOF. This was done because the dimer
4 concentration was always in the magnitude of ~1 % of monomer concentration and the trimer
5 concentration was in the magnitude of ~1 % of the dimer concentration and so on (e.g. Jokinen
6 et al. 2012). The charging efficiency might not be the same for these clusters as it is for
7 monomer. This would cause the calibration factor to change and the calculated concentration
8 to be erroneous. The uncertainty in the resulting monomer concentration is estimated to be a
9 factor of ~2. The nominal lower detection limit of CIMS and CI-API-TOF is estimated to be
10 $5 \cdot 10^4 \text{ cm}^{-3}$, and the upper limit is approximately 10^9 cm^{-3} for both instruments. At this high
11 concentration, the primary ions start to deplete causing the calibration factor to change.

12 The total sulphate concentration was measured with an online ion chromatograph MARGA 2S
13 ADI 2080. MARGA is able to detect 5 gases in the gas phase (HCl, HNO₃, HONO, NH₃, SO₂)
14 and 8 major inorganic species in aerosol phase (Cl⁻, NO₃⁻, SO₄²⁻, NH₄⁺, Na⁺, K⁺, Mg²⁺, Ca²⁺).
15 The sample flow is ~16.7 lpm. From the sample flow, all (more than 99.7 %) of water-soluble
16 gases are absorbed into a wetted rotating denuder (WRD). Based on different diffusion
17 velocities, aerosols pass the WRD and enter a Steam-Jet-Aerosol-Collector (SJAC) (Slanina et
18 al., 2001). In the SJAC, conditions are supersaturated with water vapour, which condenses onto
19 particles and the particles thus collect at the bottom of the SJAC. Sample solutions are drawn
20 from the WRD and the SJAC into syringes (25 ml) and are analysed one after another once an
21 hour. Samples are injected in cation and anion chromatographs with an internal standard (LiBr).
22 Components are detected by conductivity measurements. The detection limits are 0.1 µg m⁻³ or
23 better. For more information about the instrument, see Makkonen et al. (2012).

24 In our previous study (Brus et al., 2010), the total sulphate concentration was measured using
25 the method of bubblers: where a known flowrate from the flow tube was bubbled through
26 alkaline solution, thus trapping sulphate. This solution was then analysed using offline ion
27 chromatography. See Brus et al., (2010) for details. The method of bubbler is analogous to the
28 MARGA and the main difference is that MARGA is an online method, whilst bubbler is an
29 offline method.

30 The total-particle number concentration was measured with a Particle Size Magnifier (PSM,
31 Airmodus Oy, Finland, Vanhanen et al., 2011, coupled with CPC TSI model 3772) and with
32 Ultra-Fine CPC's (UFCPC, TSI models 3776, 3025A) with cut-off mobility diameters of ~1.5

1 nm and ~3 nm, respectively. Differential Mobility Particle Sizer (DMPS) was used to measure
2 particle number size distribution from 3 to ~250 nm in a closed-loop arrangement (Jokinen and
3 Mäkelä, 1997) using a blower to measure the wet size of the particles. The DMPS was run with
4 a sheath flow of ~11 lpm and sample flow of 1.5 lpm in the short HAUKE-type Differential
5 Mobility Analyzer (DMA). The DMA was coupled with UFCPC (TSI model 3025A) and with
6 a bipolar radioactive (^{63}Ni) neutralizer. The charging efficiencies were calculated following the
7 parameterization of Wiedensohler and Fissan (1991). The RH of the sheath flow was monitored
8 to ensure that it was same as the RH in the chamber.

9

10 **3 Results**

11 To quantify the sulphuric acid input for flow-tube nucleation measurements, the saturator
12 output was tested in two experiments: first with CIMS and CI-API-TOF and second with
13 MARGA. After the tests, nucleation measurements of sulphuric acid-water system were
14 conducted. This enabled direct comparison with the sulphuric-acid production method used in
15 our previous studies (Brus et al., 2010 and 2011), so that the production method can be
16 discounted as a reason for the discrepancy. Presented values from CIMS, CI-API-TOF and
17 MARGA measurements are residual, i.e. measured values at the end of the flow tube accounting
18 for dilutions, if not otherwise mentioned to be different.

19 **3.1 Test of the saturator**

20 Results of the saturator test are presented in Fig. 3 as measured sulphuric-acid or total-sulphate
21 concentrations and predicted values by Eq. (1) and (2) as a function of temperature of the
22 saturator. The mixing flows were 40 (dry and RH 15 %) or 20 lpm (for RH 29 %) for CIMS
23 and API-TOF and 20 lpm (only dry conditions) for MARGA measurements. Tests with
24 MARGA were performed with dry conditions, since it was noticed that the RH did not have
25 any influence on the results from the tests with mass spectrometers. MARGA uses
26 supersaturated conditions to grow the particles and collect them in the SJAC, hence initial RH
27 is not expected to have any influence. Saturator flowrate was 0.5 lpm. Mass spectrometers were
28 tested in dry and humid conditions. Dry experiments were run with two mass-spectrometer inlet
29 flowrates (6 and 10 lpm) and with extra 1 m (I.D. 4 mm) Teflon tubing between the saturator
30 and the mixing unit, to test the effect of wall losses. Humidified experiments were done with

1 two inlet flowrates (6 lpm for RH 29 % and 10 lpm for RH 15 %). MARGA experiments were
2 conducted in dry conditions.

3 The total sulphate concentration measured with MARGA (black squares) fits the prediction by
4 Eq. (2) (dashed line) very well and the prediction by Eq. (1) (solid line) underestimates the
5 measured total sulphate concentration slightly. MARGA has a relatively fast inlet flowrate
6 (~16.7 lpm) so inlet losses are low; however, with increased temperature of the saturator,
7 diffusional losses are visible.

8 Sulphuric-acid monomer concentration measured with CIMS and CI-API-TOF fit each other
9 very well, but they show one-to-two orders-of-magnitude lower concentrations than predicted
10 by Eq. (1) and (2) and measured total sulphate with MARGA. The slope is similar to the
11 predictions and to the points measured with MARGA. The dimer concentration was always
12 approximately 1 to 10 % (increasing with increasing saturator temperature) of the monomer
13 concentration and trimer approximately 1 % of the dimer concentration (see supplementary
14 material, Fig. S5).

15 Relative humidity did not have any substantial effect on the measured values by CIMS and CI-
16 API-TOF. RH can affect the wall losses by preventing the sulphuric acid's evaporation from
17 the inlet walls, since the vapour pressure of water is several orders of magnitude higher than
18 that of the sulphuric acid. The predictions by Eq. (1) and (2) do not consider relative humidity,
19 since the flow through the saturator is always dry. The relative humidity of the mixing flow
20 causes the sulphuric acid molecules to get hydrated since sulphuric acid is very hygroscopic;
21 but because the results from humid and dry measurements are very similar, CIMS and CI-API-
22 TOF can be considered to measure well in humid conditions also. The effect of RH is discussed
23 in Eisele and Tanner (1995) and our results agree with the discussion there.

24 A change of the nominal inlet flowrate of CIMS and CI-API-TOF did not have large effect. The
25 inlet lines were short (~20 cm) in the saturator tests so the wall losses due to lower inlet flowrate
26 did not play any significant role. Using instruments with a lower flowrate might alter the
27 measured concentration as the calibration factor is acquired with inlet flowrate of 10 lpm.

28 Extra saturator tests with mass spectrometers were done using three different carrier gas purities
29 (N₂ 6.0, N₂ 5.0 and pressurized air) to check if the carrier gas used in our experiments
30 (pressurized air) was more dirty than the most pure commercial ones. Two different purity
31 sulphuric acids (~97 % and 100 %) were tested also to check if the purity of the acid itself has
32 an influence. Changing the carrier gas or the sulphuric acid purity did not affect the observed

1 sulphuric-acid concentration (see supplementary material, Fig. S3 and S4). The measured
2 sulphuric-acid monomer concentration was one-to-two orders-of-magnitude lower than the
3 prediction by Eq. 1. Tests with different saturator flowrates (0.05-2 lpm) showed that with
4 flowrates below 0.1 lpm, diffusion losses dominated: causing the measured concentration to
5 decrease as a function of the saturator flowrate. Above 0.15 lpm, the observed results behaved
6 as expected. The measured cluster distributions (monomer, dimer and trimer) with different
7 carrier gas purity were constant through the measured saturator flowrate range (Fig. S5). The
8 ratios between monomer-to-dimer and dimer-to-trimer were between 1:10 and 1:100 with all
9 carrier gases. From these results it is evident that the carrier gas used in our studies does not
10 contain more contaminants than the most pure ones commercially available. CI-Api-TOF mass
11 spectra observed with different carrier gases were investigated further to find the missing
12 sulphuric acid. A large number of peaks were found to correlate with mass 97 (HSO_4^-), which
13 is the ionized sulphuric-acid monomer, with all carrier gases. The number of these peaks
14 increased as a function of the saturator temperature, suggestive that the sulphuric acid forms
15 clusters with contaminant substances (Supplementary, section 6, Fig. S6-S8). The correlating
16 peaks in Fig. S6-S8 are stick masses (i.e. rounded to nearest integer), which means that many
17 of those peaks have actually several peaks within them. This is shown in Fig. S9-S11 where the
18 mass spectrum from CI-Api-TOF is zoomed in. Unfortunately, summing up all of these
19 correlating peaks to calculate the total sulphuric acid concentration is not feasible, since these
20 clusters are not identified (i.e. it is not known what molecules those clusters are composed of)
21 and the sheer number of these peaks is overwhelming. For more details and discussion of the
22 extra saturator tests, see supplementary material.

23 **3.2 Losses of sulphuric acid and sulphate in the flow tube**

24 Total losses were not directly measured but they were determined by comparing results from
25 saturator tests with the results from nucleation measurements. The setup of the measurements
26 was similar in both experiments except for the flow tube used in nucleation measurements. By
27 accounting for the different mixing ratios of saturator flowrate and mixing flowrate, these
28 measurements become comparable and the total losses in the flow tube can be determined. The
29 Total Loss Factor (*TLF*) includes wall losses and losses to the particle phase (nucleation and
30 condensational losses).

31 Figure 4 presents the measured sulphuric-acid-monomer and total-sulphate concentration from
32 the saturator tests (squares) and nucleation measurements (stars) as a function of the saturator

1 temperature. Saturator tests were done in dry conditions and nucleation measurements in RH
2 30 %. An inlet pipe is used to connect the mass spectrometer to the flow tube. Brus et al. (2011)
3 state that the Wall Loss Factor (WLF) in the inlet pipe of length $100 + 22$ cm is $WLF_{\text{inlet}} = \sim 4$.
4 This factor, together with the mixing ratios, was accounted for to make the data sets directly
5 comparable.

6 A linear fit was applied to the data and TLF values were determined from the ratio of the fits.
7 The TLF values were determined for a saturator temperature range of 286-300 K for CIMS and
8 284-297 K for MARGA depending on the measurement range of the data. The average TLF
9 values are 14.2 ± 4.2 for CIMS and 10.0 ± 1.2 for MARGA. The R^2 values for the fits are 0.96,
10 0.87, 0.90 and 0.61 for CIMS saturator test, CIMS nucleation measurement, MARGA saturator
11 test and MARGA nucleation measurement, respectively.

12 From Fig. 4, it is evident that wall losses are not the only losses affecting the measured
13 concentrations since the trends in the fits for nucleation measurements are less steep than the
14 ones from saturator tests. The losses to the particle phase also affect the situation. The maximum
15 losses of sulphuric acid to particle phase are calculated using the DMPS data measured at the
16 end of the nucleation chamber only. The total volume of the particles is calculated within the
17 size distribution assuming that the particles are composed only of pure sulphuric acid with
18 density of 1.84 g cm^{-3} . The losses of sulphuric acid to particles range from 0 % (dry conditions,
19 $T_{\text{sat}} = 273 \text{ K}$) up to maximum of 1.4 % (RH = 30 %, $T_{\text{sat}} = 292 \text{ K}$) of the total sulphate
20 concentration. Higher saturator temperature increases the number and the diameter of the
21 particles, and relative humidity increases the diameter of the particles. The losses to the particle
22 phase are substantial at the highest values of saturator temperature but this estimate is the
23 maximum limit since the particles are not composed only of pure sulphuric-acid molecules.
24 Contaminants from the flow condense to the particle phase or bond with sulphuric acid. When
25 using humid conditions, sulphuric-acid particles uptake water since sulphuric acid is very
26 hygroscopic. At the highest temperature of the saturator, the size distribution unfortunately
27 extends out of the DMPS range (3-250 nm), thus conversely underestimating the losses. Losses
28 to the clusters smaller than the cut-off size of the particle counters are substantial. The
29 maximum losses to the particle phase have been calculated for each of the saturator temperature
30 values and plotted with the measured monomer and total sulphate concentrations together with
31 the prediction from Eq. (1) in Fig. S1 in supplementary material. Even summing up the
32 measured monomer concentration and the losses to the particle phase leaves the summed total

1 concentration at least one order of magnitude lower than the measured total sulphate and the
2 prediction by Eq. (1).

3 **3.3 Nucleation measurements**

4 Formation rates J of sulphuric acid-water were measured in the range from 0.1 to $\sim 300 \text{ cm}^{-3}\text{s}^{-1}$
5 with sulphuric acid monomer concentration approximately from $5 \cdot 10^5$ to 10^7 cm^{-3} or in total
6 sulphate concentration approximately from $4 \cdot 10^8$ to $3 \cdot 10^9 \text{ cm}^{-3}$. Formation rates are usually
7 reported as $J_{1.5}$ or J_3 (cut-off sizes of the particle counters are 1.5 nm for PSM and 3 nm for
8 UFCPC TSI models 3776 and 3025) as discussed in Kulmala et al. (2012). However, particles
9 measured at the end of our flow tube were almost always in the range of 8-20 nm, so we report
10 formation rates as they were determined with our particle counters. The purpose of these
11 nucleation measurements is to be able to compare the formation rates and the sulphuric-acid or
12 total-sulphate concentrations, between the two sulphuric-acid vapour-production methods. The
13 results are discussed below.

14 Figure 5 presents DMPS and CIMS data for one cycle of saturator temperatures. Panel a)
15 presents the number size distribution as a function of time, panel b) the total particle number
16 concentration, panel c) shows the hourly averaged sulphuric-acid monomer concentration with
17 standard deviation as the error bars and panel d) shows hourly averaged saturator temperature.
18 One can see from Fig. 5, panels a) and b), that when the temperature of the saturator changes,
19 the number concentration and the number size distribution are not stable immediately. The
20 sulphuric-acid concentration overshoots slightly at the beginning whilst the system stabilizes to
21 steady state. The first hour of averages from each of the saturator temperatures was excluded
22 to ensure only steady-state data ($\text{std}(T) = \pm 0.05 \text{ K}$) were included in the averages. When a new
23 cycle started, the T_{sat} dropped from the maximum value ($\sim 315 \text{ K}$) to the minimum (273 K)
24 causing a long period of unstable data, and the first two hours were excluded from the beginning
25 of the cycle. In panel a) in Fig. 5, nucleation is the main process below temperature of $\sim 290 \text{ K}$
26 and growth takes over at higher temperatures. This can be seen as the bimodal distribution at
27 highest saturator temperatures.

28 Figures 6 and 7 present the number concentration N_{exp} (panel a)), geometric mean diameter D_p
29 (panel b)) and apparent formation rate J (panel c)) of freshly nucleated particles with sulphuric-
30 acid monomer concentration [H_2SO_4 monomer] or total sulphate [SO_4^{2-}] (panel d)) as a function
31 of saturator temperature T_{sat} for nucleation temperature of 298 K with several different relative

1 humidity values (Fig. 6) and saturator flowrates (Fig. 7). The formation rate is reported the
2 observed particle concentration N_{exp} divided by the residence time τ .

3 From Fig. 6, it is evident that all measured variables behave as expected as a function of the
4 saturator temperature, except for the apparent saturation of the observed particle concentration
5 (and hence, the formation rate). PSM was coupled with the TSI model 3772 CPC's, which has
6 an upper limit of 10^4 cm^{-3} for the particle concentration. This caused the observed particle
7 concentration to saturate in Fig. 6, even though the particle concentration was confirmed to
8 increase to higher values by DMPS data (not shown in the Fig. 6). Coagulation has a minor
9 effect on the particle number due to a short residence time ($\tau = 30 \text{ s}$) and relatively low particle
10 concentration. The relative humidity affects mostly the diameter of the particles, but also
11 decreasing RH decreases the formation rate if similar sulphuric acid concentration is
12 considered. A lower formation rate with decreased RH might be caused by the diminishing of
13 the particle diameter below the detection limit of the UFCPC (TSI model 3776). In Fig. 7, the
14 squares present measurements during dry conditions and stars during RH of 30 %. Panel d)
15 shows also the detection limit of MARGA for total sulphate concentration. The detection limit
16 was determined from 20 hours of measurements with saturator flowrate set to zero and averaged
17 over the time period. The detection limit was $1.35 \cdot 10^9 \text{ cm}^{-3}$. All the total sulphate concentrations
18 measured below this detection limit were considered as erroneous and rejected from further
19 analysis, even though these values are presented in Fig. 7. MARGA can be used with
20 concentration columns to measure lower concentrations of species but it was not available in
21 this study.

22 From Fig. 7, one can see that all the variables responded in a similar manner as CIMS and CI-
23 Api-TOF experiment (Fig. 6). As the temperature of the saturator approaches the temperature
24 of the mixing unit (laboratory temperature, $\sim 294 \text{ K}$) the number concentration of particles
25 decreases and starts to increase again when saturator temperature is greater than that of the
26 mixing unit. This is an artefact of the setup.

27 The main difference between Fig. 6 and 7 is the maximum diameter reached. Due to the greater
28 maximum saturator temperature (315 K) in the experiment with the mass spectrometers, the
29 maximum diameter reached up to $\sim 130 \text{ nm}$ compared to the $\sim 23 \text{ nm}$ with the experiment with
30 MARGA. The residence times in the flow tube are the same in both experiments ($\sim 30 \text{ s}$). The
31 measured sulphuric-acid monomer concentration is at typical atmospheric levels, but the
32 growth rates are much higher: indicating higher concentration of sulphuric-acid-containing

1 condensing vapour than the detected sulphuric-acid-monomer concentration by CIMS. The
2 growth is rather driven by the total sulphate, originating exclusively from the sulphuric acid
3 inside the saturator, than the sulphuric-acid-monomer concentration.

4 To show the contribution of the sulphate to the growth rate, the model described in Škrabalová
5 et al. (2014) was used to calculate the diameter (D_p) and growth rate (GR) of the particles.
6 Measured sulphuric-acid monomer and total-sulphate concentrations (Fig. 6 and 7, panel d),
7 RH 30 %) were multiplied by the $TLFs$ to obtain the initial concentrations of vapour at the
8 beginning of the flow tube. Diameter of 1.5 nm was chosen as the initial cluster size according
9 to Kulmala et al. (2007). The model was used with three scenarios of particle neutralization by
10 ammonia: (0) no neutralization, particles composed of sulphuric acid and water, (1)
11 neutralization to ammonium bisulphate-water particles and (2) neutralization to ammonium
12 sulphate-water particles. When accounting for the initial sulphuric-acid monomer concentration
13 as an input, the resulting diameter (D_p) was always below 2 nm with growth rates (GR) ranging
14 approximately from 1 to 15 nm h⁻¹ as a function of the sulphuric-acid concentration (i.e.
15 saturator temperature T_{sat}) with all scenarios. When total-sulphate concentration was used as an
16 input, the resulting particle diameters and growth rates fit well with the measured particle
17 diameters presented in Fig. 7 for all scenarios (see suppl. Material, section 7 and Fig. S12).

18 **3.4 Formation rates and comparison to our previous results**

19 Figure 8 presents formation rates J of the H₂SO₄-H₂O system as a function of sulphuric-acid
20 monomer concentration measured with CIMS at nucleation temperature of $T = 298$ K and RH
21 of ~30 %. Sulphuric acid was produced with the method of furnace (red squares, Brus et al.,
22 2011) and with saturator (the black squares, present study). The sulphuric-acid concentration
23 for data from Brus et al. (2011) is presented here as residual concentration (i.e. at the end of the
24 flow tube) so that these two measurements would be comparable. Brus et al. (2011) present
25 their data as the initial concentration. Both datasets have almost identical slopes (1.3 and 1.2)
26 and the formation rates J have a difference of a factor of 2. For the dataset measured with the
27 production method of the furnace, the residence time ($\tau = 15$ s) is defined as the time that the
28 particles spend in the flow tube after the nucleation zone. The nucleation zone was
29 experimentally determined (Brus et al., 2010) and confirmed with CFD model (Herrmann et
30 al., 2010) to be in the middle of the flow tube in the measurements with the furnace, where a
31 thermal gradient was present. For the saturator measurements (present work), the residence time
32 ($\tau = 30$ s) was defined as the whole time the particles spend in the flow tube. The difference of

1 the residence time is exactly a factor of 2. Formation rate is defined as the number concentration
2 divided by the residence time, so these two sets of data lie on top of each other if the same
3 residence time would have been used for formation-rate determination.

4 Figure 9 presents formation rates J of $\text{H}_2\text{SO}_4\text{-H}_2\text{O}$ as a function of residual total sulphate
5 concentration $[\text{SO}_4^{2-}]$ at RH of $\sim 30\%$ and at nucleation temperature of $T = 298\text{ K}$. Stars are the
6 data from measurements where sulphuric-acid vapour was produced with the furnace and total
7 sulphate measured with bubbler method (Brus et al., 2010). The residence time used in there
8 was $\tau = 15\text{ s}$. Squares are total sulphate measured with MARGA in this study with different
9 flowrates through the saturator, and the residence time was $\tau = 30\text{ s}$. All the points have the
10 standard deviation as error bars. The detection limit of MARGA is also marked as a dashed
11 vertical line. Formation rates are similar with both production methods. As previously, the
12 factor of two difference in the residence time increases the scatter between the two datasets.

13 Figures 8 and 9 show that apparent formation rates are reproducible with both sulphuric-acid
14 production methods, with similar observed sulphuric-acid or total-sulphate concentrations. This
15 eliminates the sulphuric-acid production method as a reason for the discrepancy between the
16 measured monomer and total sulphate concentrations. The data are more scattered in Fig. 9 due
17 to the larger integration times used in MARGA and bubbler measurements. During several
18 hours of integration time, a small change in flowrates can cause a substantial difference in the
19 resulting concentration. MARGA data are close to the detection limit of the instrument, which
20 also causes larger scatter.

21 Figure 10 shows comparison of the apparent formation rates J as a function of residual
22 sulphuric-acid monomer $[\text{H}_2\text{SO}_4\text{ monomer}]$ or total sulphate concentration $[\text{SO}_4^{2-}]$ from this
23 study to our previous studies with the standard deviation as error bars. Note the difference of a
24 factor of two between the residence times. Squares show values measured using mass
25 spectrometers (PSM, red and black squares; TSI 3776, green squares). Stars are data measured
26 using ion-chromatograph (i.e. total sulphate) methods with two different UFCPC's (TSI 3025A,
27 black stars and TSI 3776, red stars). Figure 10 shows that the production method does not have
28 substantial effect since the results lie on same line when comparing results obtained with mass
29 spectrometers or MARGA and bubbler method. The conditions for all the measurements were
30 similar ($T = 298\text{ K}$, RH $\sim 30\%$).

31 The slope of the data measured using MARGA or bubblers is steeper than the slope of the
32 results measured with mass spectrometers. There is a discrepancy of one-to-two orders-of-

1 magnitude between sulphuric-acid monomer and total-sulphate concentration for similar
2 formation rates. The UFCPC 3776 (green squares) was probably undercounting at the lowest
3 sulphuric acid concentrations. This can be seen in Fig. 10 where the lowest observed formation
4 rates are not consistent with the rest of the data. This is probably caused by the small size of the
5 particles at such low sulphuric-acid concentration ($1\text{-}2\cdot 10^6\text{ cm}^{-3}$) (Sipilä et al., 2010).

6 The comparison to literature data was omitted in this manuscript as the formation rates in the
7 present study are very similar to our previous results (Brus et al., 2010 and 2011). However, for
8 comparison and review of experimental data on sulphuric-acid nucleation, we refer to Zollner
9 et al., (2012) and Zhang et al., (2012).

10 **3.5 Contaminants**

11 In our previous study (Brus et al., 2011), an ion chromatograph was used to determine the
12 background levels of ammonia and it was found that the background concentration was below
13 the detection limit of the IC (500 pptv), accounting for the flowrates in the nucleation chamber.
14 The concentration of background ammonia was measured with the MARGA system in this
15 study. An average total concentration (gas and particle phase) of ammonia was 60 pptv for dry
16 conditions and 126 pptv for RH 30 %, supporting our previous results. The concentration did
17 not change as a function of saturator temperature, thus it is assumed to originate from the
18 purified, particle-free air used as carrier gas in all measurements and the ultrapure water (Milli-
19 Q, Millipore) used for humidification. The concentration for dry conditions is in the same order
20 of magnitude as the concentration of total sulphate at the lowest (273 K) temperature of the
21 saturator. When increasing the saturator temperature, ammonia to total sulphate-ratio decreases
22 from ~1:1 to ~1:10 or less for dry conditions and from ~3:1 to ~1:5 for humid conditions. The
23 extra saturator tests, mentioned in section 3.1 and found in supplementary material, showed that
24 the carrier gas used in this experiment was at least as pure as the most pure gas available
25 commercially (AGA, N₂, 6.0), which has impurities less than 1 ppm, including hydrocarbons
26 less than 0.1 ppm. According to the results found in supplementary material, the actions taken
27 to purify the carrier gas in these experiments were sufficient. Nevertheless, there were
28 contaminants left in the carrier gas at levels which will affect the nucleation process.

29

1 4 Discussion and Conclusions

2 A saturator was used to produce sulphuric-acid vapour from neat-liquid sulphuric acid for
3 laboratory studies. It was tested and shown to produce similar apparent formation rates at
4 similar conditions to our previous vapour-production method of the furnace. The sulphuric-acid
5 or total-sulphate concentration was measured with two independent methods and it was shown
6 to produce exact concentrations as prediction from Richardson et al. (1986) and slightly higher
7 than the prediction from Kulmala and Laaksonen (1990) when measured with MARGA (Fig.
8 3). Concentrations of sulphuric-acid monomer measured with CIMS and CI-Api-TOF was one-
9 to-two orders-of-magnitude lower than the total-sulphate values measured with MARGA and
10 the prediction by Eq. (1) and (2). The only source of sulphuric acid (sulphate measured by
11 MARGA) is the liquid sulphuric acid inside the saturator as seen in Fig. 3. A possible reason
12 for the discrepancy is that the sulphuric acid is in particle phase since the saturator is a
13 substantial source of particles. However, these particles are lost on the way from the saturator
14 to the nucleation chamber due to two main reasons: (i) the flowrate (0.5 lpm) in the tube (length:
15 1 m, I.D. 4 mm) from the saturator to the nucleation chamber is relatively low increasing
16 diffusional losses and (ii) the highly turbulent mixing of the saturator flow with the mixing flow
17 ($Q_{sat} : Q_{mix} \approx 1:30$ or more) transforms the mixer into an effective trap for the particles. The loss
18 of the particles is confirmed with DMPS measurements which cannot explain the discrepancy
19 (supplementary material, Fig. S1). Maximum losses to the particle phase in the flow tube are 0-
20 1.4 % with an average below 1 % of the total sulphate. The discrepancy cannot be explained by
21 the formation of larger clusters containing solely sulphuric acid (dimer, trimer, etc.) either,
22 because the concentration of these clusters is in the order of few percent or lower than the
23 monomer concentration (Supplementary material, Fig. S5).

24 The characteristics of the freshly nucleated particles together with the conditions used for the
25 nucleation has been identified and presented (Fig. 4-7). Total losses of sulphuric acid or total
26 sulphate to the whole flow-tube setup have been determined for both methods to detect the
27 concentration of sulphuric acid or total sulphate.

28 The average Total Loss Factors determined are $TLF = 10.0 \pm 1.2$ ($T_{sat} = 284-297$ K) for
29 MARGA and $TLF = 14.2 \pm 4.2$ ($T_{sat} = 286-300$ K) for CIMS both having a slight increasing
30 deviation from the first-order losses as a function of saturator temperature (Fig. 4). The second-
31 order losses are caused by losses to the particles and losses to the clusters which are too small
32 to be detected by particle counters.

1 Formation rates of sulphuric acid-water system were compared to our previous studies (Brus et
2 al., 2010 and 2011), where a method of the furnace was used (Fig. 8-10). Obtained apparent
3 formation rates as a function of sulphuric-acid or total-sulphate concentrations were
4 independent of the sulphuric-acid vapour-production method (furnace vs saturator). Conditions
5 for these studies were similar ($T = 298$ K, RH ~ 30 %) but at similar formation rates, the
6 sulphuric-acid monomer concentration is one-to-two orders-of-magnitude lower than the total
7 sulphate. The slope of the fit to the formation-rate data as a function of sulphuric-acid monomer
8 concentration (1.3 ± 0.2) is very similar as obtained in Brus et al. (2011) (1.2 ± 0.1). The
9 comparison to our previous measurements was done to check reproducibility of the nucleation-
10 experiment results between the sulphuric-acid vapour-production methods and to eliminate the
11 production method as a possible reason for the discrepancy. The discussion and interpretation
12 of the slopes (section 3.1) and comparison to the atmospheric data (section 3.5) can be found
13 in Brus et al. (2011).

14 Average ammonia concentration of 60 pptv was found in the system for dry conditions and 126
15 pptv for RH 30 % as a contaminant and it was independent of the saturator temperature. It is
16 assumed to originate from the purified, dry, particle-free air used as carrier gas and from the
17 ultrapure water used for humidifying the mixing flow. Ammonia concentration is enough to
18 affect the nucleation process itself substantially but the magnitude of this effect was not studied
19 in this work. Ammonia can bind sulphuric acid by forming clusters, which might reduce the
20 monomer concentration measured with CIMS and CI-API-TOF slightly. Since the contaminant
21 level was constant and saturator temperature was increased, reducing the contaminant to total
22 sulphate-ratio from $\sim 1:1$ to $\sim 1:10$ for dry conditions and from $\sim 3:1$ to $\sim 1:5$ for humid conditions,
23 does not explain the discrepancy between the two sulphuric-acid- or total-sulphate-detection
24 methods. Even though the contaminant levels might sound high, those are still below the most-
25 pure commercially available gases (AGA, N₂, 6.0).

26 Other possible reasons for the difference between sulphuric acid monomer and total sulphate is
27 that sulphuric acid molecules are most probably bonded to some molecule(s) (e.g. amines,
28 ammonia, organics) and not detected by CIMS or identified from the CI-API-TOF spectra
29 (Kulmala et al., 2013). As Kurten et al. (2011) state, base molecules can be only in minor
30 importance due to the fact that nitrate ion (NO₃⁻) will most probably substitute the base out in
31 the CIMS charging process. Nevertheless, there is expected to be a substantial pool of clusters
32 formed of sulphuric acid-base molecules in our system, which are too small to be detected by

1 current state-of-art particle counters such as PSM. These clusters are the main reason for the
2 discrepancy between measured total-sulphate and the monomer concentrations. Same or similar
3 clusters are most probably forming in all laboratory nucleation experiments involving sulphuric
4 acid, as there are always contaminants present in carrier gases. Further analysis of the CI-Api-
5 TOF mass spectra showed a large number of stick-unit masses correlating with sulphuric-acid
6 monomer ion (HSO_4^-) suggesting a large number of clusters containing sulphuric acid which
7 are not used for calculating the sulphuric-acid concentration measured by mass spectrometers
8 (see supplementary material, section 6 and Fig. S6-S11). Sulphuric acid (measured here as
9 sulphate) can contribute to the early growth of ultrafine particles to a much larger extent than
10 currently thought, since most of the sulphuric acid remains undetected. Also the huge number
11 of correlating masses with increasing sulphuric-acid concentration implies that there are
12 numerous substances that can form stable clusters with sulphuric acid that may be the starting
13 point for particle formation.

14 The total sulphate (originally total sulphuric acid) is responsible for the particle growth as
15 demonstrated in Skrabalova et al. (2014). The contribution of the total sulphate to the nucleation
16 process itself is not yet fully understood. However, recent results suggest that sulphuric acid
17 monomer is the main component in nucleation (Brus et al., 2014) and not the overall sulphuric
18 acid. To find out which molecules are possibly involved in nucleation, the clusters with
19 sulphuric acid must be identified from the CI-Api-TOF spectra.

20

21 **Acknowledgements**

22 The financial support by the Academy of Finland Centre of Excellence program (project no.
23 1118615), KONE foundation and by the Maj and Tor Nessling Foundation are gratefully
24 acknowledged. The language improvements provided by Curtis Wood are gratefully
25 acknowledged.

26

27

28

29

30

1 **References**

- 2 Arnold., F.: Ion-induced nucleation of atmospheric water vapor at the mesopause, *Planetary*
3 *and Space Science*, 28, 10, 1003-1009, doi: 10.1016/0032-0633(80)90061-6, 1980.
- 4 Ayers, G. P., Gillett, R. W. and Gras, J. L.: On the vapor pressure of sulphuric acid, *Geophys.*
5 *Res. Letters*, 7, 6, 433-436, 1980.
- 6 Ball, S. M., Hanson, D. R. and Eisele, F. L.: Laboratory studies of particle nucleation: Initial
7 results for H₂SO₄, H₂O, and NH₃ vapors, *J. of Geophys. Res.*, 104, D19, 23,709-23,718, doi:
8 10.1029/1999JD900411, 1999.
- 9 Benson, D., Young, L.-H., Kameel, F. and Lee, S.-H.: Laboratory-measured nucleation rates of
10 sulfuric acid and water binary homogeneous nucleation from the SO₂ + OH reaction, *Geophys.*
11 *Res. Lett.*, 35, L11801, doi:10.1029/2008GL033387, 2008.
- 12 Benson, D. R., Erupe, M. E. and Lee, S.-H.: Laboratory-measured H₂SO₄-H₂O-NH₃ ternary
13 homogeneous nucleation rates: Initial observations, *Geophys. Res. Letters*, 36, L15818,
14 doi:10.1029/2009GL038728, 2009.
- 15 Benson, D. R., Yu, J. H., Markovich, A. and Lee, S.-H.: Ternary homogeneous nucleation of
16 H₂SO₄, NH₃, and H₂O under conditions relevant to the lower troposphere, *Atmos. Chem. Phys.*,
17 11, 4755-4766, doi: 10.5194/acp-11-4755-2011, 2011.
- 18 Berndt, T., Stratmann, F., Bräsel, S., Heintzenberg, J., Laaksonen, A. and Kulmala, M.: SO₂
19 oxidation products other than H₂SO₄ as a trigger of new particle formation. Part 1: Laboratory
20 investigations, *Atmos. Chem. Phys.*, 8, 6365-6374, 2008.
- 21 Berndt, T., Stratmann, F., Sipilä, M., Vanhanen, J., Petäjä, T., Mikkilä, J., Gruner, A., Spindler,
22 G., Lee Mauldin III, R., Curtius, J., Kulmala, M. and Heintzenberg, J.: Laboratory study on
23 new particle formation from the reaction OH + SO₂: influence of experimental conditions, H₂O
24 vapour, NH₃ and the amine tert-butylamine on the overall process, *Atmos. Chem. Phys.*, 10,
25 7101-7116, doi:10.5194/acp-10-7101-2010, 2010.
- 26 Berresheim, H., Elste, T., Plass-Dülmer, C. Eisele, F. L. and Tanner, D. J.: Chemical ionization
27 mass spectrometer for long-term measurements of atmospheric OH and H₂SO₄, *Int. J. of Mass*
28 *Spectr.* 202, 91-109, 2000.

1 Brus, D., Hyvärinen, A.-P., Viisanen, Y., Kulmala, M. and Lihavainen H.: Homogeneous
2 nucleation of sulfuric acid and water mixture: experimental setup and first results, *Atmos.*
3 *Chem. Phys.*, 10, 2631-2641, 2010.

4 Brus, D., Neitola, K., Petäjä, T., Vanhanen, J., Hyvärinen, A.-P., Sipilä, M., Paasonen, P.,
5 Lihavainen H. and Kulmala, M.: Homogenous nucleation of sulfuric acid and water at
6 atmospherically relevant conditions, *Atmos. Chem. Phys.*, 11, 5277-5287, doi:10.5194/acp-11-
7 5277-2011, 2011.

8 Brus, D., Hyvärinen, A.-P., Anttila, T., Neitola, K., Koskinen, J., Makkonen, U., Hellén, H.,
9 Hemmilä, M., Sipilä, M., Mauldin III, R. L., Jokinen, T., Petäjä, T., Kurtén, T., Vehkamäki, H.,
10 Kulmala, M., Viisanen, Y., Lihavainen, H., and Laaksonen, A.: Reconsidering the sulphuric
11 acid saturation vapour pressure: Classical Nucleation Theory revived, *Physical Review Letters*,
12 in review, (2014).

13 Davidson, C., Phalen, R. and Solomon P.: Airborne Particulate Matter and Human Health: a
14 Review, *Aerosol Sci. and Tech.*, 39, 8, 2005.

15 Eisele, F. and Tanner, D.: Measurement of the gas phase concentration of H₂SO₄ and methane
16 sulfonic acid and estimates of H₂SO₄ production and loss in the atmosphere, *J. Geophys. Res.*,
17 98, D5, 9001-9010, doi:10.1029/93JD00031, 1993.

18 Feingold G. and Siebert, H.: Chapter 14 Cloud-Aerosol Interactions from the Micro to the
19 Cloud Scale, in *Clouds in the Perturbed Climate System*, edited by J. Heintzenberg and R.J.
20 Charlson, pp. p. 576, The MIT Press, Cambridge, 2009.

21 Herrmann, E., Brus, D., Hyvärinen, A.-P., Stratmann, F., Wilck, M., Lihavainen, H. and
22 Kulmala, M.: A computational fluid dynamics approach to nucleation in the water-sulfuric acid
23 system, *J. Phys. Chem. A*, 114 (31), 8033-8042, 2010.

24 Hirsikko, A., Nieminen, T., Gagné, S., Lehtipalo, K., Manninen, H. E., Ehn, M., Hörrak, U.,
25 Kerminen, V.-M., Laakso, L., McMurry, P. H., Mirme, A., Mirme, S., Petäjä, T., Tammet, H.,
26 Vakkari, V., Vana, M. and Kulmala, M.: Atmospheric ions and nucleation: a review of
27 observations, *Atmos. Chem. Phys.*, 11, 767-798, doi:10.5194/acp-11-767-2011, 2011.

28 Jokinen, V. and Mäkelä, J. M.: Closed-loop arrangement with critical orifice for DMA sheath/
29 excess flow system. *J. Aerosol Sci.*, 28, 643-648, 1997.

1 Jokinen, T., Sipilä, M., Junninen, H., Ehn, M., Lönn, G., Hakala, J., Petäjä, T., Mauldin III, R.
2 L., Kulmala, M., and D. R. Worsnop, D. R.: Atmospheric sulphuric acid and neutral cluster
3 measurements using CI-API-TOF. *Atmos. Chem. Phys.*, 12, 4117-4125, doi:10.5194/acp-12-
4 4117-2012, 2012.

5 Junninen, H., Ehn, M., Petäjä, T., Luosujärvi, L., Kotiaho, T., R. Kostianen, R., Rohner, U.,
6 Gonin, M., Fuhrer, K., Kulmala, M. and Worsnop, D.: A high-resolution mass spectrometer to
7 measure atmospheric ion composition, *Atmos. Meas. Tech.*, 3, 1039-1053, doi:10.5194/amt-3-
8 1039-2010, 2010.

9 Kerminen, V.-M. Petäjä, T., Manninen, H. E., Paasonen, P., Nieminen, T., Sipilä, M., Junninen,
10 H., Ehn, M., Gagné, S., Laakso, L., Riipinen, I., Vehkamäki, H., Kurten, T., Ortega, I. K., Dal
11 Maso, M., Brus, D., Hyvärinen, A.-P., Lihavainen, H., Leppä, J., Lehtinen, K. E. J., Mirme, A.,
12 Mirme, S., Horrák, U., Berndt, T., Stratmann, F., Birmili, W., Wiedensohler, A., Metzger, A.,
13 Dommen, J., Baltensperger, U., Kiendler-Scharr, A., Mentel, T. F., Wildt, J., Winkler, P. M.,
14 Wagner, P. E., Petzold, A., Minikin, A., Plass-Dülmer, C., Pöschl, U., Laaksonen, A. and M.
15 Kulmala, M.: Atmospheric nucleation: highlights of the EUCAARI project and future
16 directions, *Atmos. Chem. Phys.*, 10, 10829-10848, doi:10.5194/acp-10-10829-2010, 2010.

17 Kirkby, J., Curtius, J., Almeida, J., Dunne, E., Duplissy, J., Ehrhart, S., Franchin, A., Gagné,
18 S., Ickes, L., Kürten, A., Kupc, A., Metzger, A., Riccobono, F., Rondo, L., Schobesberger,
19 S., Tsagkogeorgas, G., Wimmer, D., Amorim, A., Bianchi, F., Breitenlechner, M., David, A.,
20 Dommen, J., Downard, A., Ehn, M., Flagan, R., Haider, S., Hansel, A., Hauser, D., Jud, W.,
21 Junninen, H., Kreissl, F., Kvashin, A., Laaksonen, A., Lehtipalo, K., Lima, J., Lovejoy, E.,
22 Makhmutov, V., Mathot, S., Mikkilä, J., Minginette, P., Mogo, S., Nieminen, T., Onnela, A.,
23 Pereira, P., Petäjä, T., Schnitzhofer, R., Seinfeld, J., Sipilä, M., Stozhkov, Y., Stratmann, F.,
24 Tomé, A., Vanhanen, J., Viisanen, Y., Aron Vrtala, A., Wagner, P., Walther, H., Weingartner,
25 E., Wex, H., Winkler, P., Carslaw, K., Worsnop, D., Baltensperger, U. and Kulmala, M.: Role
26 of sulphuric acid, ammonia and galactic cosmic rays in atmospheric aerosol nucleation, *Nature*,
27 476, 429-433, doi:10.1038/nature10343, 2011.

28 Korhonen, P., Kulmala, M., Laaksonen, A., Viisanen, Y., McGraw, R., and Seinfeld, J. H.:
29 Ternary nucleation of H₂SO₄, NH₃ and H₂O in the atmosphere, *J. Geophys. Res.*, 104, 26 349-
30 26 353, doi: 10.1029/1999JD900784, 1999.

1 Kulmala M. and Laaksonen, A.: Binary nucleation of water-sulfuric acid system: Comparison
2 of classical theories with different H₂SO₄ saturation vapor pressures, *J. Chem. Phys.*, 93 (1). 1,
3 doi: 10.1063/1.459519, 1990.

4 Kulmala, M., Vehkamäki H., Petäjä T., Dal Maso M., Lauri A., Kerminen V.-M., Birmili W.
5 and McMurry P. H.: Formation and growth rates of ultrafine atmospheric particles: A review
6 of observations, *J. Aerosol Sci.*, 35, 143-176, doi: 10.1016/j.jaerosci.2003.10.003, 2004a.

7 Kulmala, M., Lehtinen, K. E. J., and Laaksonen, A.: Cluster activation theory as an explanation
8 of the linear dependence between formation rate of 3 nm particles and sulphuric acid
9 concentration, *Atmos. Chem. Phys.*, 6, 787-793, 2006.

10 Kulmala, M., Riipinen, I., Sipilä, M., Manninen, H. E., Petäjä, T., Junninen, H., Dal Maso, M.,
11 Mordas, G., Mirme, A., Vana, M., Hirsikko, A., Laakso, L., Harrison, R. M., Hanson, I., Leung,
12 C., Lehtinen, K. E. J., Kerminen, V.-M.: Towards direct measurement of atmospheric
13 nucleation, *Science*, 318, 89, DOI: 10.1126/science.1144124, 2007.

14 Kulmala, M., Petäjä, T., Nieminen, T., Sipilä, M., Manninen, H. E., Lehtipalo, K., Dal Maso,
15 M., Aalto, P. P., Junninen, H., Paasonen, P., Riipinen, I., Lehtinen K. E. J., Laaksonen Kari E
16 J and Kerminen, V-M.: Measurement of the nucleation of atmospheric aerosol particles, *Nature*
17 *protocols*, 7, 9, doi:10.1038/nprot.2012.091, 2012.

18 Kulmala, M., Kontkanen, J., Junninen, H., Lehtipalo, K., Manninen, H. E., Nieminen, T.,
19 Petäjä, T., Sipilä, M., Schobesberger, S., Rantala, P., Franchin, A., Jokinen, T., Järvinen, E.,
20 Äijälä, M., Kangasluoma, J., Hakala, J., Aalto, P. P., Paasonen, P., Mikkilä, J., Vanhanen, J.,
21 Aalto, J., Hakola, H., Makkonen, U., Ruuskanen, T., Mauldin III, R. L., Duplissy, J.,
22 Vehkamäki, H., Bäck, J., Kortelainen, A., Riipinen, I., Kurten, T., Johnston, M. V., Smith, J.
23 N., Ehn, M., Mentel, T. F., Lehtinen, K. E. J., Laaksonen, A., Kerminen, V.-M. and Worsnop,
24 D. R.: Direct observations of atmospheric aerosol nucleation, *Science*, 339, 6122, 943-946,
25 2013.

26 Kürten, A., Rondo, L., Ehrhart, S. and Curtius, J.: Calibration of a Chemical Ionization Mass
27 Spectrometer for the Measurement of Gaseous Sulfuric Acid, *J. Phys. Chem. A*, 116, 6375-
28 6386, 2012.

29 Lee, S.-H., Reeves, J. M., Wilson, J. C., Hunton, D. E., Viggiano, A. A., Miller, T. M.,
30 Ballenthin, J. O., Lait, L. R.: Particle Formation by Ion Nucleation in the Upper Troposphere
31 and Lower Stratosphere, *Science*, 301, 5641, 1886-1889, doi: 10.1126/science.1087236, 2003.

1 Lovejoy, E. R., Curtius, J., and Froyd, K. D.: Atmospheric ion-induced nucleation of sulphuric
2 acid and water, *J. Geophys. Res.*, 109, D08204, doi:10.1029/2003JD004460, 2004.

3 Lihavainen, H., Kerminen, V.-M., Komppula, M., Hatakka, J., Aaltonen, V., Kulmala, M. and
4 Viisanen Y.: Production of “potential” cloud condensation nuclei associated with atmospheric
5 new-particle formation in northern Finland, *J. Geophys. Res.*, 108(D24), 4782,
6 doi:10.1029/2003JD003887, 2003.

7 Makkonen, U., Virkkula, A., Mäntykenttä, J., Hakola, H., Keronen, P., Vakkari, V. and Aalto,
8 P. P.: Semi-continuous gas and inorganic aerosol measurements at a Finnish urban site:
9 comparisons with filters, nitrogen in aerosol and gas phases, and aerosol acidity, *Atmos. Chem.*
10 *Phys.*, 12, 5617-5631, doi:10.5194/acp-12-5617-2012, 2012.

11 Manninen, H. E., Nieminen, T., Asmi, E., Gagné, S., Häkkinen, S., Lehtipalo, K., Aalto, P.,
12 Vana, M., Mirme, A., Mirme, S., Hörrak, U., Plass-Dülmer, C., Stange, G., Kiss, G., Hoffer,
13 A., Törö, N., Moerman, M., Henzing, B., de Leeuw, G., Brinkenberg, M., Kouvarakis, G. N.,
14 Bougiatioti, A., Mihalopoulos, N., O’Dowd, C., Ceburnis, D., Arneth, A., Svenningsson, B.,
15 Swietlicki, E., Tarozzi, L., Decesari, S., Facchini, M. C., Birmili, W., Sonntag, A.,
16 Wiedensohler, A., Boulon, J., Sellegri, K., P. Laj, P., Gysel M., Bukowiecki, N., Weingartner,
17 E., Wehrle, G., Laaksonen, A., Hamed, A., J. Joutsensaari, J., Petäjä, T., Kerminen, V.-M. and
18 Kulmala, M.: EUCAARI ion spectrometer measurements at 12 European sites - analysis of new
19 particle formation events, *Atmos. Chem. Phys.*, 10, 7907-7927, doi: 10.5194/acp-10-7907-
20 2010, 2010.

21 Mauldin III, R. L., Frost, G., Chen, G., Tanner, D., Prevot, A., Davis, D., and Eisele, F.: OH
22 measurements during the First Aerosol Characterization Experiment (ACE 1): Observations
23 and model comparisons, *J. Geophys. Res.*, 103, 16713-16729, doi:10.1029/98JD00882, 1998.

24 Merikanto, J., Spracklen, D. V., Mann, G. W., Pickering, S. J., and Carslaw, K. S.: Impact of
25 nucleation on global CCN, *Atmos. Chem. Phys.*, 9, 8601-8616, 2009.

26 Napari, I., Noppel, M., Vehkamäki, H. and Kulmala M.: Parametrization of ternary nucleation
27 rates for $\text{H}_2\text{SO}_4\text{-NH}_3\text{-H}_2\text{O}$ vapors, *J. Geophys. Res.*, 107(D19), 4381,
28 doi:10.1029/2002JD002132, 2002.

29 Nieminen, T., Paasonen, P., Manninen, H. E., Sellegri, K., Kerminen, V.-M. and Kulmala, M.:
30 Parameterization of ion-induced nucleation rates based on ambient observations, *Atmos. Chem.*
31 *Phys.*, 11, 3393-3402, doi:10.5194/acp-11-3393-2011, 2011.

1 Paasonen, P., Nieminen, T., Asmi, E., Manninen, H. E., Petäjä, T., Plass-Dülmer, C., Flentje,
2 H., Birmili, W., Wiedensohler, A., Horrák, U., Metzger, A., Hamed, A., Laaksonen, A.,
3 Facchini, M. C., Kerminen, V.-M. and Kulmala, M.: On the roles of sulphuric acid and low-
4 volatility organic vapours in the initial steps of atmospheric new particle formation, *Atmos.*
5 *Chem. Phys.*, 10, 11223-11242, doi:10.5194/acp-10-11223-2010, 2010.

6 Petäjä, T., Mauldin, III, R., Kosciuch, E., McGrath, J., Nieminen, T., Paasonen, P., Boy, M.,
7 Adamov, A., Kotiaho, T. and Kulmala M.: Sulfuric acid and OH concentrations in a boreal
8 forest site, *Atmos. Chem. Phys.*, 9, 7435-7448, 2009.

9 Richardson, C. B., Hightower, R. L. and Pigg, A. L.: Optical measurements of evaporation of
10 sulphuric acid droplets, *Applied Optics*, 25, 7, 1226-1229, 1986.

11 Sipilä, M., Berndt, T., Petäjä, T., Brus, D., Vanhanen, J., Stratmann, F., Patokoski, J., Mauldin
12 III, Roy L., Hyvärinen, A.-P., Lihavainen, H. and Kulmala, M.: The role of sulphuric acid in
13 atmospheric nucleation, *Science*, 327, 5970, 1243-1246, doi: 10.1126/science.1180315, 2010.

14 Škrabalová L., Brus, D., Anttila, T., Ždímal, V. and Lihavainen H.: Growth of sulphuric acid
15 nanoparticles under wet and dry conditions, *Atmos. Chem. Phys.* 14, 6461-6475,
16 doi:10.5194/acp-14-6461-2014, 2014.

17 Slanina, J., ten Brink, H. M., Otjes, R. P., Even, A., Jongejan, P., Khlystov, S., Waijers-Ijpelaan,
18 A., Hu, M., and Lu, Y.: The continuous analysis of nitrate and ammonium in aerosols by the
19 steam jet aerosol collector (SJAC): extension and validation of the methodology, *Atmos.*
20 *Environ.*, 35, 2319-2330, doi:10.1016/S1352-2310(00)00556-2, 2001.

21 Spracklen, D. V., Carslaw, K. S., Kulmala, M., Kerminen, V.-M., Mann, G. W. and Sihto, S.
22 L.: The contribution of boundary layer nucleation events to total particle concentration on
23 regional and global scales, *Atmos. Chem. Phys.*, 6, 5631-5648, 2006.

24 ten Brink, H., Otjes, R., Jongejan, P. and Slanina S.: An instrument for semi-continuous
25 monitoring of the size-distribution of nitrate, ammonium, sulphate and chloride in aerosol,
26 *Atmos. Environ.*, 41, 13, 2768-2779, 10.1016/j.atmosenv.2006.11.041, 2007.

27 Vanhanen, J., Mikkilä, J., Lehtipalo, K., M. Sipilä, M., Manninen, H., Siivola, E., Petäjä, T.
28 and Kulmala, M.: *Aerosol Sci. and Tech.*, 45, 4, 533-542, doi:10.1080/02786826.2010.547889,
29 2011.

1 Vehkamäki, H., Kulmala, M., Napari, I., Lehtinen, K. E. J., Timmreck, C., Noppel, M. and
2 Laaksonen A.: An improved parameterization for sulfuric acid-water nucleation rates for
3 tropospheric and stratospheric conditions, *J. Geophys. Res.*, 107(D22), 4622,
4 doi:10.1029/2002JD002184, 2002.

5 Viisanen, Y., Kulmala, M. and Laaksonen, A.: Experiments on gas-liquid nucleation of sulfuric
6 acid and water, *J. Chem. Phys.* 107, 920; doi: 10.1063/1.474445, 1997.

7 Weber, R. J., Marti, J. J., McMurry, P. H., Eisele, F. L., Tanner, D. J. and Jefferson, A.:
8 Measured atmospheric new particle formation rates: Implications for nucleation mechanisms,
9 *Chemical Engineering Communications*, 151, 53-64, doi: 10.1080/00986449608936541, 1996.

10 Wiedensohler, A. and Fissan, H. J.: Bipolar Charge Distributions of Aerosol Particles in High-
11 Purity Argon and Nitrogen, *Aerosol Sci. and Tech.*, 14:358-364, doi:
12 10.1080/02786829108959498, 1991.

13 Winkler, P. M., Steiner, G., Vrtala, A., Vehkamäki, H., Noppel, M., Lehtinen, K. E. J., Reischl,
14 G. P., Wagner, P. E., Kulmala, M.: Heterogeneous Nucleation Experiments Bridging the Scale
15 from Molecular Ion Clusters to Nanoparticles, *Science*, 319, 5868,1374-1377, doi:
16 10.1126/science.1149034, 2008.

17 Wyslouzil, B. E., Seinfeld, J. H. and Flagan, R. C.: Binary nucleation in acid-water systems. I.
18 Methanesulfonic acid-water, *J. Chem. Phys.* 94, 6842, 1991.

19 Young, L., Benson, D., Kameel, F., Pierce, J., Junninen, H., Kulmala, M. and Lee, S.-H.:
20 Laboratory studies of H₂SO₄/H₂O binary homogeneous nucleation from the SO₂+OH reaction:
21 evaluation of the experimental setup and preliminary results, *Atmos. Chem. Phys.*, 8, 4997-
22 5016, 2008.

23 Yu, F.: From molecular clusters to nanoparticles: second-generation ion-mediated nucleation
24 model, *Atmos. Chem. Phys.*, 6, 5193-5211, 2006.

25 Yu, F., Wang, Z., Luo, G. and Turco R.: Ion-mediated nucleation as an important global source
26 of tropospheric aerosols, *Atmos. Chem. Phys.*, 8, 2537-2554, 2008.

27 Yu, F.: Ion-mediated nucleation in the atmosphere: Key controlling parameters, implications,
28 and look-up table, *J. of Geophys. Res.*, 115, D03206, doi:10.1029/2009JD012630, 2010.

29 Zhang, R., Khalizov, A. F., Wang, L., Hu, M., Xu, W.: Nucleation and growth of nanoparticles
30 in the atmosphere, *Chem. Rev.* 112, 1957-2011, doi: 10.1021/cr2001756 2012.

1 Zheng, J., Khalizov, A., Wang, L. and Zhang, R.: Atmospheric Pressure-Ion Drift Chemical
2 Ionization Mass Spectrometry for Detection of Trace Gas Species, *Anal. Chem.*, 82, 7302-7308,
3 doi: 10.1021/ac101253n, 2010.

4 Zollner, J. H., Glasoe, W. A., Panta, B., Carlson, K. K., McMurry, P. H. and Hanson, D. R.:
5 Sulfuric acid nucleation: power dependencies, variation with relative humidity, and effect of
6 bases, *Atmos. Chem. Phys.*, 12, 4399-4411, doi:10.5194/acp-12-4399-2012, 2012.

7

8

9

10

11

12

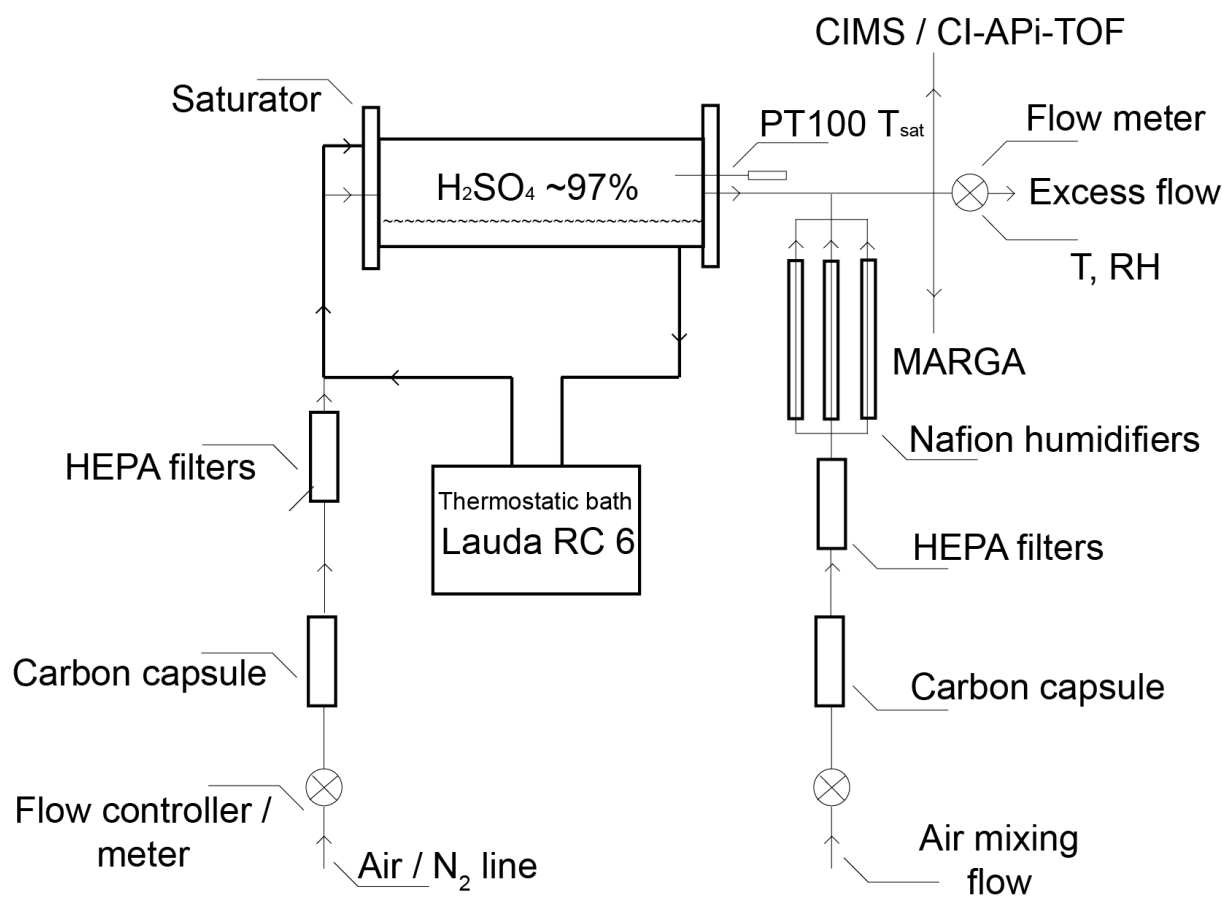
13

14

15

16

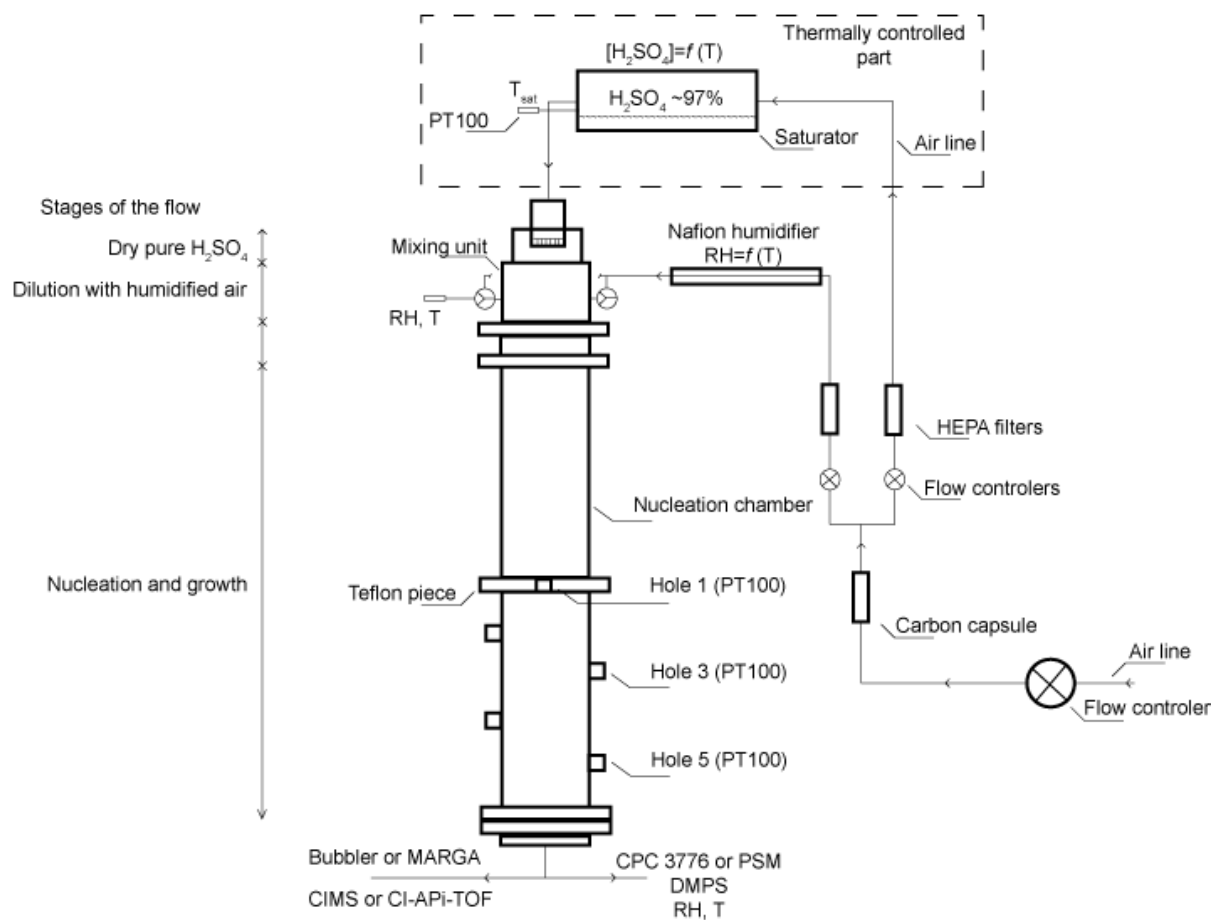
17



1

2

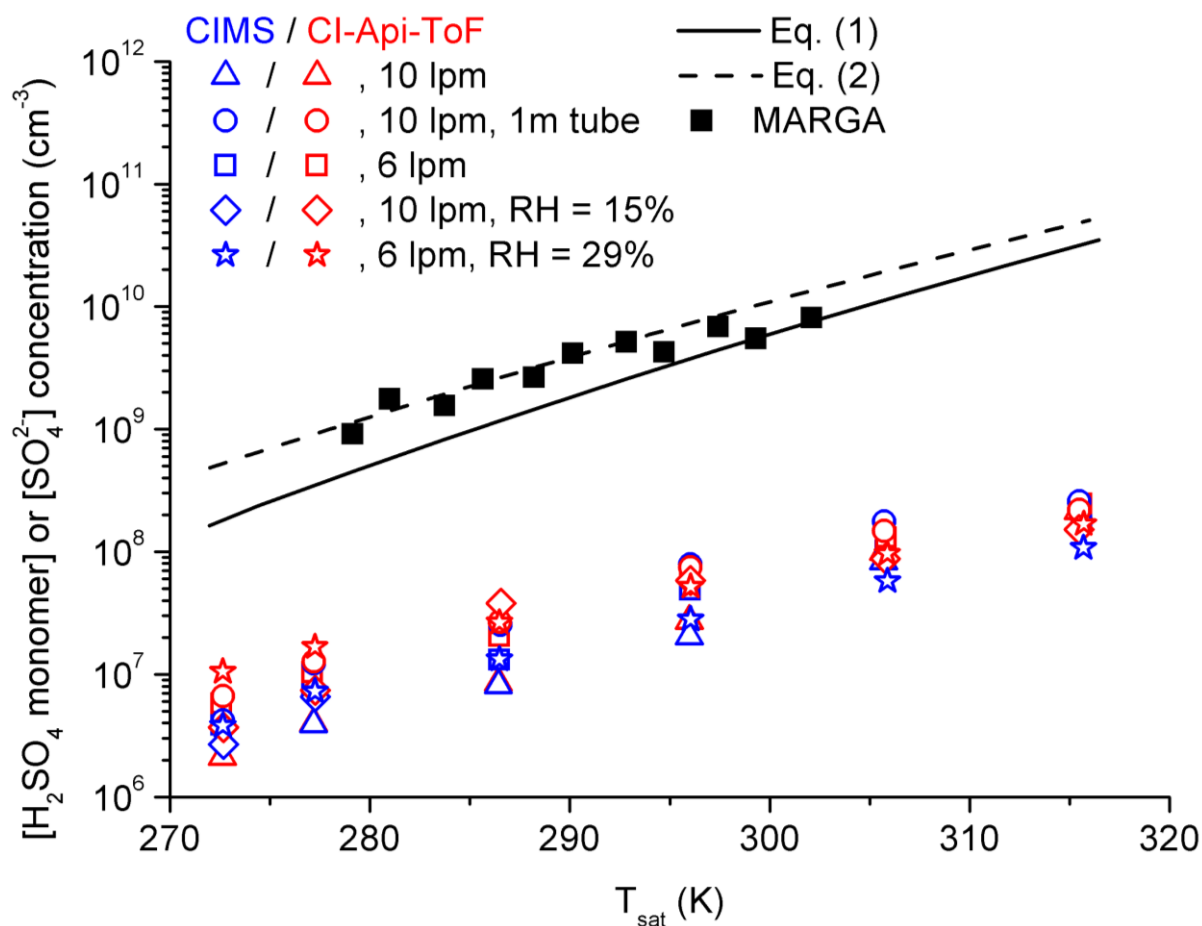
3 Figure 1. Schematic figure of the setup for testing the saturator.



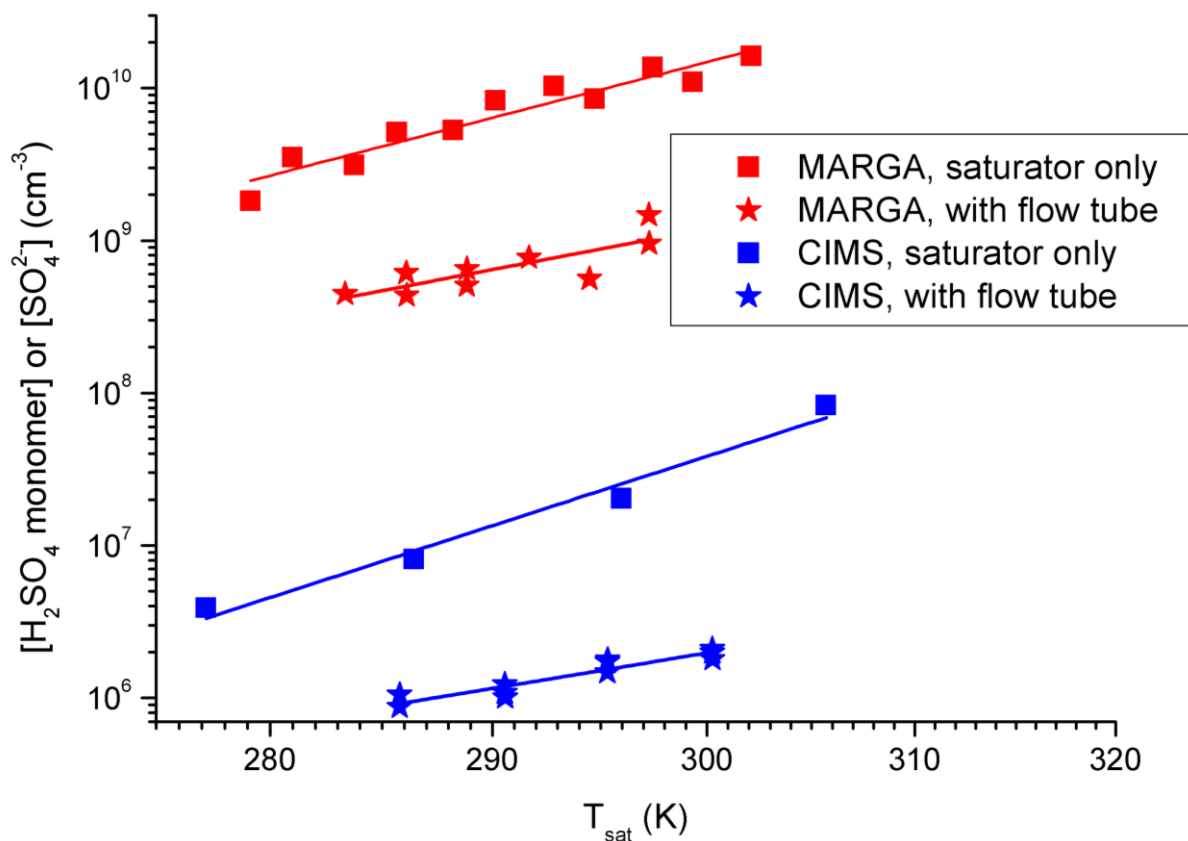
1

2

3 Figure 2. Flow-tube setup.



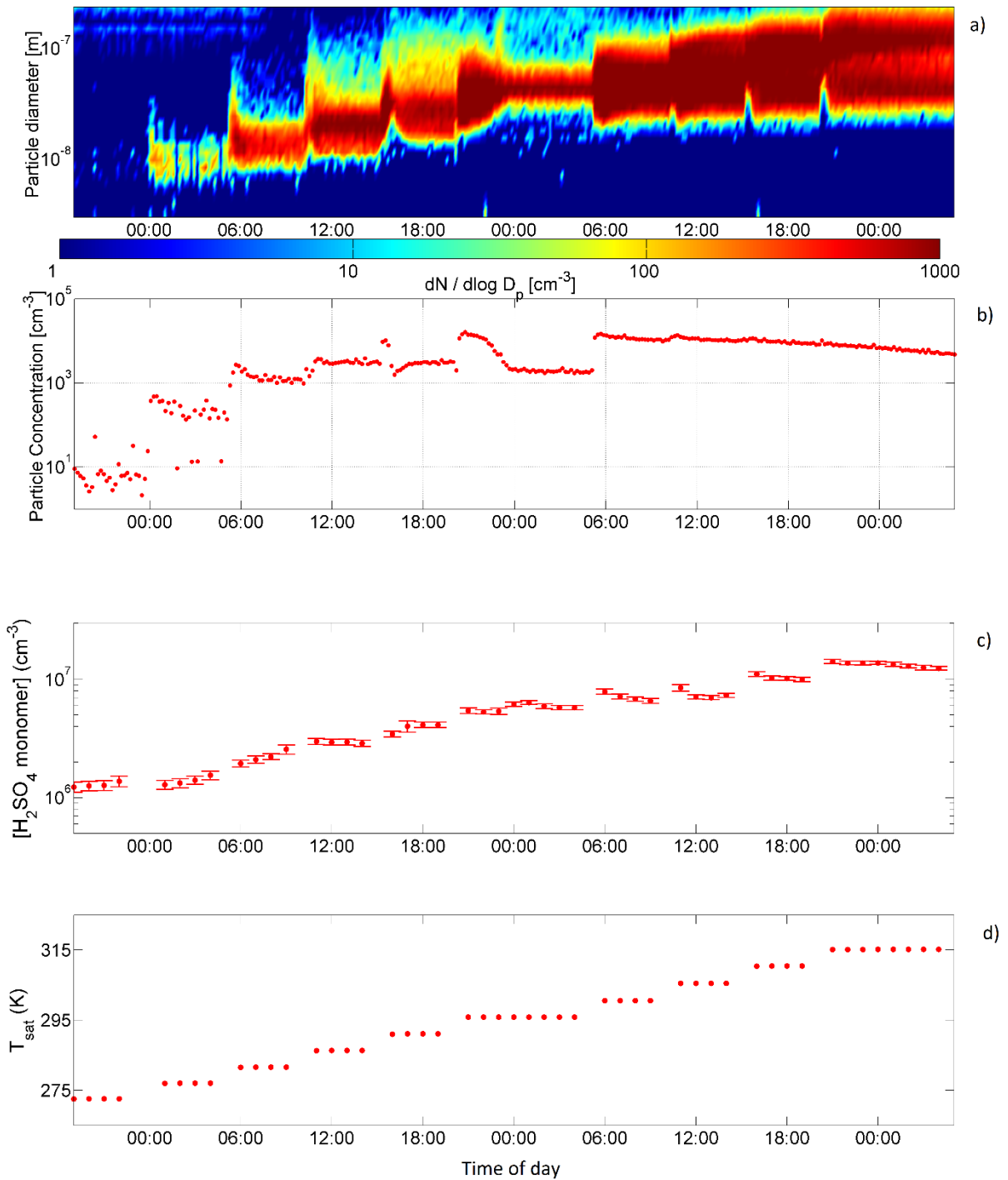
1
2
3 Figure 3. Measured sulphuric-acid monomer $[H_2SO_4 \text{ monomer}]$ and total-sulphate $[SO_4^{2-}]$
4 (black squares) concentrations together with predicted values by Eq. (1) and (2) as a function
5 of saturator temperature T_{sat} . Saturator flowrate is $Q_{sat} = 0.5$ lpm and mixing flowrates were 40
6 lpm (dry for CIMS and CI-Api-TOF and RH 15 %) and 20 lpm (MARGA and RH 29 %). CIMS
7 (blue markers) and CI-Api-TOF (red markers) have been tested with 6 lpm and 10 lpm
8 (nominal) inlet total flowrates and also with an extra 1 m Teflon tubing after saturator.



1

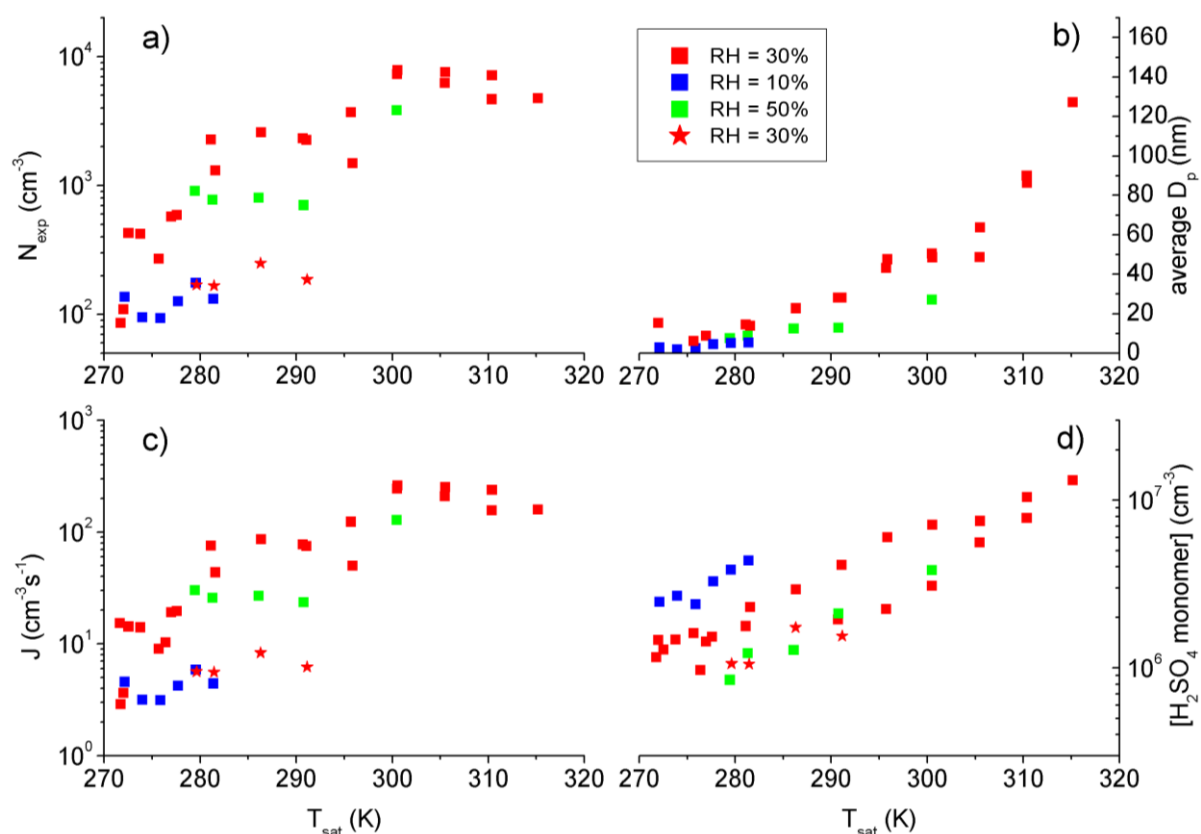
2

3 Figure 4. Comparison of MARGA and CIMS data between test with only saturator (dry
 4 conditions, squares) and with saturator and flow tube (RH ~30 %, stars). Different flowrates
 5 through saturator have been accounted for. Average total loss factors are $TLF_{\text{MARGA}} = 10.0 \pm$
 6 1.2 and $TLF_{\text{CIMS}} = 14.2 \pm 4.2$. See text for details.

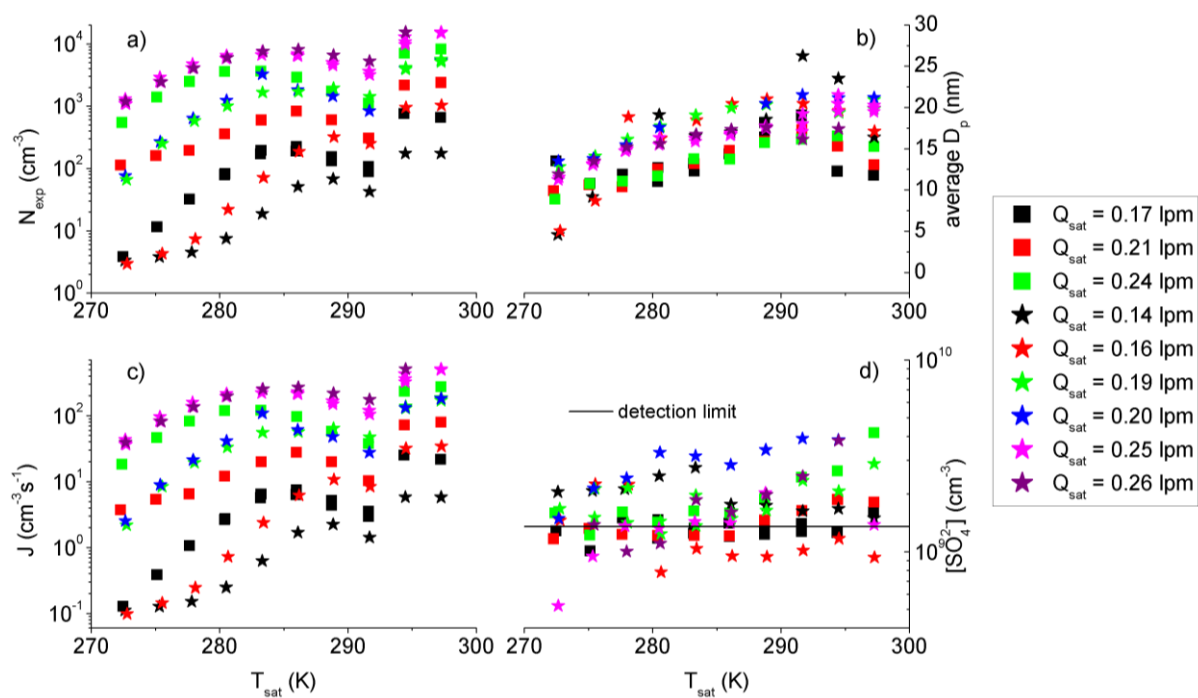


1
2

3 Figure 5. DMPS and CIMS data from one T_{sat} cycle. Panel a) shows the number size
4 distribution, panel b) shows the total number concentration from DMPS, panel c) shows the
5 CIMS-measured sulphuric-acid monomer concentration averaged over one hour with standard
6 deviation as error bars and panel d) shows hourly averaged temperature of the saturator.



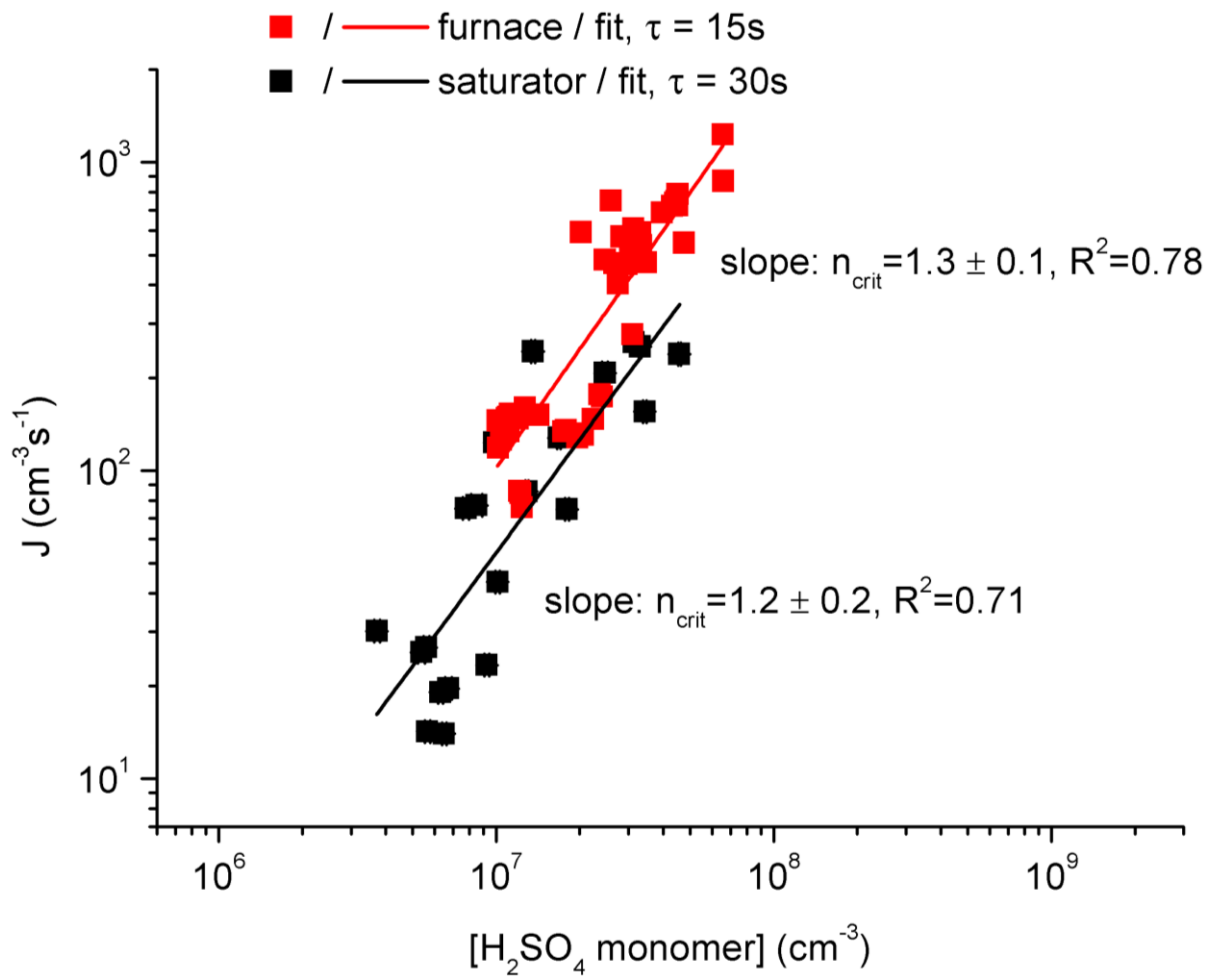
1
2
3 Figure 6. Number concentration N_{exp} (panel a)) measured with PSM and TSI 3776, geometric-
4 mean diameter D_p (panel b)), apparent formation rate J (panel c)) of the freshly nucleated
5 particles and sulphuric-acid monomer concentration measured (panel d)) with CIMS (squares)
6 or CI-API-TOF (stars) with several relative humidity as a function of saturator temperature with
7 saturator flow of 0.1 lpm. All data are averaged over a period of constant saturator temperature
8 excluding first hour to ensure steady-state. Stars are measured with CI-API-TOF and squares
9 with CIMS. All data are averaged over a period of constant saturator temperature (± 0.05 K)
10 extracting first hour.



1

2

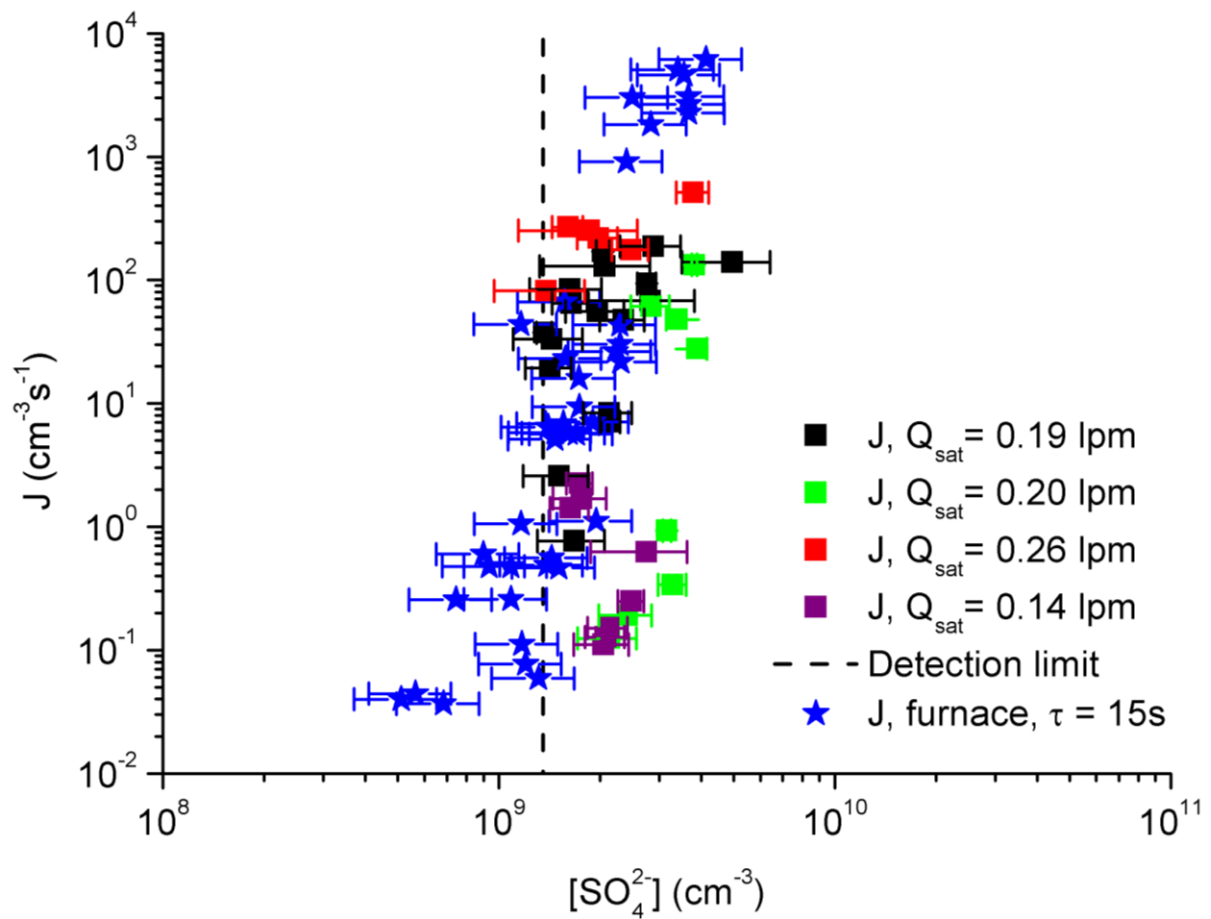
3 Figure 7. Number concentration N_{exp} (panel a)) measured with TSI 3776, geometric mean
 4 diameter D_p (panel b)), formation rate J (panel c)) of the freshly nucleated particles and total-
 5 sulphate concentration from MARGA (panel d)) with detection limit of MARGA with several
 6 different saturator flowrates as a function of saturator temperature. Squares represent
 7 measurements at dry conditions, stars are measured with RH of $\sim 30\%$. All data are averaged
 8 over a period of constant saturator temperature (± 0.05 K) extracting first hour.



1

2

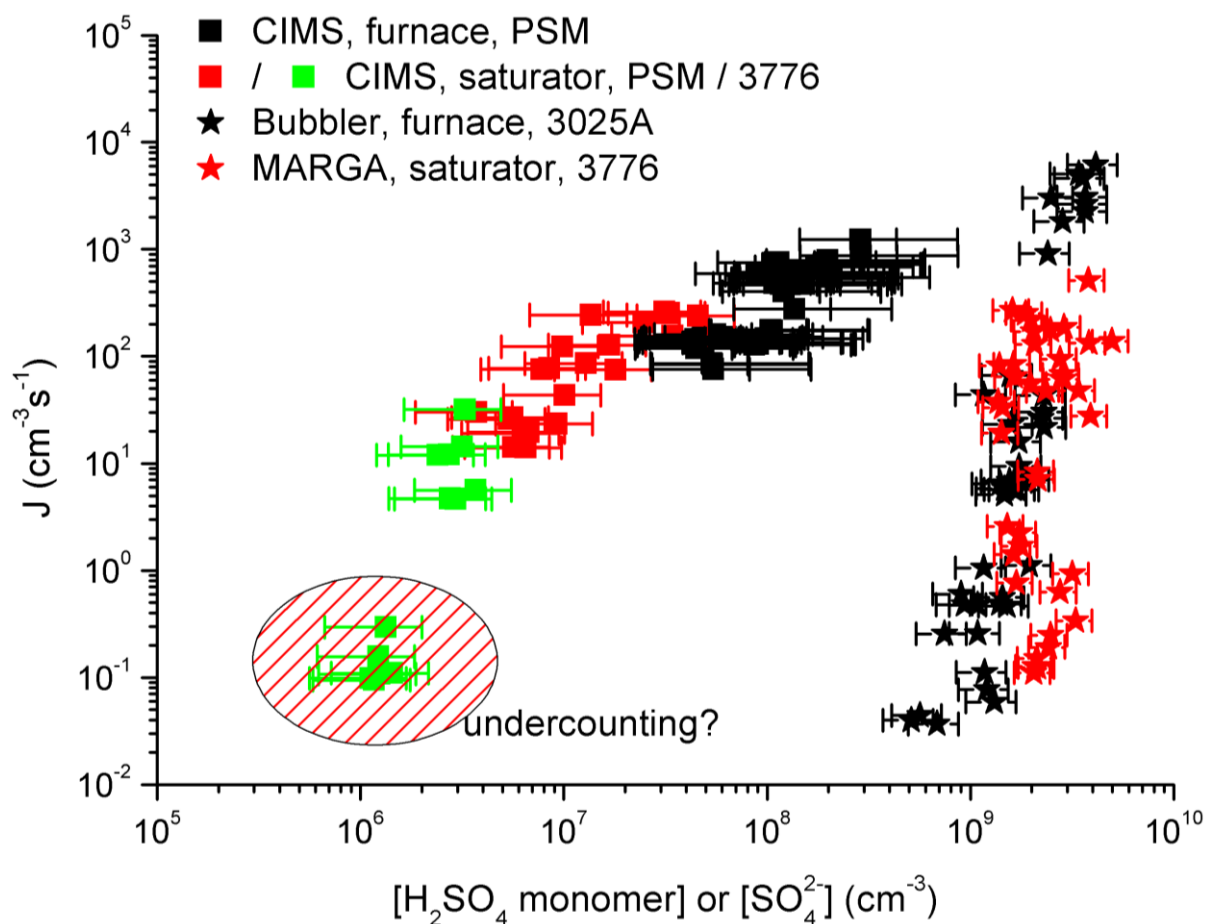
3 Figure 8. Formation rates J as a function of residual sulphuric acid monomer concentration
 4 $[\text{H}_2\text{SO}_4 \text{ monomer}]$ at $T = 298 \text{ K}$ and $\text{RH} \sim 30 \%$ measured using CIMS. In the first dataset
 5 (red squares) sulphuric-acid vapour was produced with the furnace method and the residence
 6 time was defined to be 15 s (Brus et al., 2011).



1

2

3 Figure 9. Formation rates J as a function of total-sulphate concentration $[SO_4^{2-}]$ measured
 4 with MARGA or bubbler with different saturator flowrates. MARGA's detection limit is
 5 marked with the dashed line. Relative humidity RH \sim 30 % and nucleation temperature $T =$
 6 298 K. Sulphuric-acid vapour was produced with the furnace method (Brus et al., 2010) for
 7 bubbler measurements and with the saturator method for MARGA.



1
 2
 3 Figure 10. Comparison of formation rates J as a function of residual sulphuric-acid monomer
 4 concentration $[\text{H}_2\text{SO}_4]$ or total-sulphate concentration $[\text{SO}_4^{2-}]$ to our previous results.
 5 Conditions are similar ($T = 298 \text{ K}$, $\text{RH} \sim 30 \%$). Note the factor-of-two difference between the
 6 residence times between furnace and saturator measurements. Sulphuric-acid vapour was
 7 previously produced with the furnace method and total sulphate concentration measured with
 8 the bubbler method (Brus et al., 2010).